Master's thesis

NTNU
Norwegian University of Science and Technology
Faculty of Medicine and Health Sciences
Kavli Institute for Systems Neuroscience

Ece Gozde Demirci

Visual and tactile representation of social interactions in mouse secondary motor and anterior cingulate cortices

Master's thesis in Neuroscience
Supervisor: Jonathan Whitlock
September 2019

NTNU
Norwegian University of
Science and Technology

Ece Gözde Demirci

Visual and tactile representation of social interactions in mouse secondary motor and anterior cingulate cortices

Master's Thesis in Neuroscience
Supervisor: Jonathan Whitlock
Co-supervisor: Karoline Hovde
Trondheim, September 2019

Norwegian University of Science and Technology
Faculty of Medicine and Health Sciences
Kavli Institute for Systems Neuroscience

NTNU
Kunnskap for en bedre verden

Acknowledgements

The work presented in this thesis was carried out at the Kavli Institute for Systems Neuroscience/Centre for Neural Computation at NTNU and partly at McKnight Brain Institute at University of Florida, under the supervision of Jonathan Whitlock.

First and foremost, I would like to thank Jonathan for welcoming me to the group and being an awesome mentor. Thank you for believing in me and trusting me to achieve a collaborative project overseas. It was a unique experience for a master's project and I deeply appreciate it.

I would like to thank Sara Burke and Drew Maurer for welcoming me to their home and being amazing hosts. Sara, thank you for accepting me to your lab and having infinite patience and kindness. The time I spent in Gainesville was short and hectic yet an overall incredible experience. Rest of the Burke Lab, it was a pleasure to meet you. I would like to extend my sincere gratitude to Katelyn for her great assistance in my project and SJ for inviting me to her home and letting me spend time with Percy the Super Cat. He was a supreme companion.

Next, I would like to thank Karoline Hovde for her valuable guidance and willingness to teach me all about mice. To the rest of the Whitlock Group, you all made this past year a great adventure. Tuce, thank you for being ready to provide support and all the help with the practicalities of the experiment. It was always a pleasure to catch a quick chat with you. Bartul, you are awesome and deserving of many thanks. I am forever grateful for your help and support in analysis and visualization. I appreciated the brainstorming sessions and your unique approach to matters.

Thank you all my friends who extended their support and understanding along the way and made this adventure all the more worthwhile. Gerard, Ecem and Nazli thanks for letting me vent and calming me down when I needed. Tugce, you were an amazing flatmate. Thank you for taking care of me and feeding me when I was too worn out to do so.

Finally, I would like to thank my family, my parents Fahriye and Ahmet Demirci, my siblings Esra and Emre. Thank you for supporting this life choice and letting me have an amazing journey thousands of miles away from home. I feel lucky to have you as my family and I love you all.

Abstract

Visual and tactile representation of social interactions in mouse secondary motor and anterior cingulate cortices

Secondary motor (M2) and anterior cingulate (ACC) cortices are frontal association areas in the rodent brain that receive substantial information from several primary and associative areas, including visual and posterior parietal cortices. Rodent M2 is thought to be homologous to monkey premotor, supplementary motor and frontal eye areas, and is associated with self-initiated action and whisker movements.

The anterior cingulate cortex in rodents, on the other hand, is strongly associated with pain architecture and observational fear learning. Evidence suggests that ACC in rats exhibits mirror neuron-like activation for observed and experienced pain, and that it is critical for vicarious fear learning in rats and mice. However, much less is known of rodent ACC function in the context of prosocial behaviour, even though human and monkey studies suggest the ACC is important for social cognition, including emotional regulation in a social context and during positive social interactions.

Rodents also rely heavily on tactile information, especially via whisking behaviour, to sense objects in the world and each other. In both mice and rats, physical touch with a conspecific facilitates social buffering of pain, consolation, and it has been shown to have anxiolytic effects. Both M2 and ACC are therefore likely to play important roles for tactile processing and are suitable candidates for social cognition research.

Therefore, we wished to determine if voluntary physical interaction with a conspecific drove preferential activity in M2 or ACC compared to interactions that did not allow tactile interaction. To do this we used fluorescence in situ hybridization (FISH) against the immediate early gene *Arc* to compare activity patterns of neural ensembles across two behavioural epochs of social interaction with a conspecific. One of the epochs allowed voluntary physical interaction while the second epoch was confined to visual observation.

We hypothesized that tactile *versus* visual interactions would lead to differentiated representations in both M2 and ACC, and this activity shift would be reflected in the distributed pattern of *Arc* signal. Our results, however, did not match this prediction. Rather, the data suggested that M2 and ACC respond to both types of social interaction with a general elevation in activity instead of separate ensembles. These results are consistent with a general role of these areas in processing social interactions regardless of whether the signals involved are only visual or include direct physical contact.

Contents

Acknowledgements iii
Abstract v
Abbreviations ix
Introduction 1
1.1 Motor Cortex and Mirror Neurons 1
1.2. Rodent Models of Social Cognition 2
1.3. Secondary Motor Cortex 4
1.3.1 Anatomy of the Secondary Motor Cortex 4
1.3.2 Connectivity of Secondary Motor Cortex 5
1.3.3 Functions of Secondary Motor Cortex 6
1.4 Anterior Cingulate Cortex (ACC) 8
1.4.1 Anatomy of the Anterior Cingulate Cortex 8
1.4.2 Connectivity of Anterior Cingulate Cortex 10
1.4.3 Functions of Anterior Cingulate Cortex 12
1.5 Cellular Compartment Analysis of Temporal Activity by Fluorescent in Situ Hybridization (catFISH) 14
1.5.1 Immediate Early Genes 14
1.5.2 Immediate Early Gene *Arc* (Activity Regulated Cytoskeleton Protein) 15
1.5.3 CatFISH 15
1.6 Aim 17
Methods and Materials 19
2.1 Behaviour and Animals 19
2.1.1 Animals 19
2.1.2 Experimental Set-up 20
2.1.3 Behaviour Experiment Design 20
2.2 Tissue Preparation 22
2.2.1 Maximum Electroconvulsive Shock 22
2.2.2 Snap Freezing 22
2.2.3 Sectioning 23
2.3 In Situ Hybridization and Staining Procedures 23
2.3.1 DAPI Staining 23
2.3.2 Section Selection and Delineation 24
2.3.3 In situ Hybridization 24

2.4 Imaging and Processing 26
2.4.1 Imaging the Samples 26
2.4.2 Cell Counting for Analysis 28
2.5 Methods Workflow 30
2.6 Data Analysis and Statistics 31
2.6.1 Behavioural Scoring from Experiment Videos 31
2.6.2 Statistics 31
Results 33
3.1 Interaction and Observation 33
3.2 Main Cell Count 34
3.3 Arc Signal Distribution 35
3.3.1 Comparison of Experimental Animals (EXP) to Cage Controls (CC) 35
3.3.2 *Arc* Distribution Comparisons Across Brain Regions in Experimental Animals 37
3.3.3 Similarity Scores 38
Discussion 41
4.1 Summary of the Results 41
4.2 Methodological Considerations 42
4.3 Discussion of Results 43
4.3.1 Interaction and Social Status 43
4.3.2 Social Interaction Activates Secondary Motor and Anterior Cingulate Cortices 44
4.3.3 Novel Contexts Activate Secondary Motor and Anterior Cingulate Cortices 46
4.3.4 Secondary Motor and Anterior Cingulate Cortices were Activated to Differing Degrees 47
4.3.5 Similarity Scores 47
4.4 Functional Implications 48
4.5 Limitations 49
4.6 Future Directions 50
Conclusion 53
Bibliography 55
APPENDIX 61
Appendix A – Vendor List for chemicals, reagents, etc. 61
Appendix B – Solution recipes 62
Appendix C – FISH protocols 63
Appendix D – Software Used for Data Collection and Analysis 65
Appendix E – Supplementary Material 66

Abbreviations

ACC – Anterior cingulate cortex

BLA – Basolateral nucleus of amygdala

dACC – Dorsal anterior cingulate cortex

dmPFC –dorsomedial prefrontal cortex

M1 – Primary motor cortex

M2 – Secondary motor cortex

PPC – Posterior parietal cortex

PL – Prelimbic cortex

RSC – Retrosplenial cortex

vACC – Ventral anterior cingulate cortex

Figure 2 Abbreviations

ACAd – Dorsal anterior cingulate cortex

ACAv – Ventral anterior cingulate cortex

CLA – Claustrum

ECT – Ectorhinal area

ENTm – Entorhinal cortex, medial part

ILA – Infralimbic area

MOs – Secondary motor cortex

ORBm – Orbital area, medial part

ORBvl – Orbital area, ventrolateral part

ORBl – Orbital area, lateral part

PERI – Perirhinal area

PL – Prelimbic area

PTLp – Posterior parietal association areas

RSPv – Retrosplenial area, ventral part

RSPd – Retrosplanial area, dorsal part

RSPagl – Retrosplenial area, lateral agranular part

SUBd – Dorsal subiculum

SSp – Primary somatosensory area

SSp bfd.c – Primary somatosensory area, barrel field, caudal domain

SSp tr – Primary somatosensory area, trunk

SSp II – Primary somatosensory area, lower limb

TEa - Temporal association areas

Figure 4 Abbreviations

24a – Ventral anterior cingulate cortex

24b – Dorsal anterior cingulate cortex

24a' – Ventral midcingulate cortex

24b' – Dorsal midcingulate cortex

MO – Medial orbital cortex

VO – Ventral orbital cortex

LO – Lateral orbital cortex

AI – Agranular insular cortex

M1 – Primary motor cortex

M2 – Secondary motor cortex

S1 – Primary somatosensory cortex

S2 – Secondary somatosensory cortex

PtA – Parietal associative cortex

Au – Primary auditory cortex

TeA – Temporal association cortex

EcT – Ectorhinal cortex

PRh – Perirhinal cortex

V1 – Primary visual cortex

V2M – Secondary visual cortex

CA1 – Amon's horn 1

MS – Medial septal nucleus

VDB – Diagonal band of Broca, vertical limb

HDB – Diagonal band of Broca, horizontal limb

GP – Globus pallidus

VP – Ventral pallidum

Cl – Claustrum

BLA – Basolateral amygdaloid nucleus, anterior

Chapter 1
Introduction

Social cognition is fundamental for survival throughout the animal kingdom. Many species, including humans, are prosocial animals, and many important life skills are derived from the perception and interpretation of how and when other members of the society act in certain situations. These skills can range from do-or-die actions, such as perception and avoidance of a predator, finding sustenance or a mate, as well as more advanced tools in human societies such as language development.

Social cognition and empathy are important for interpreting the mental and motivational states of others, and they facilitate the gathering of social cues that allow for imitation and observational learning.

In humans, the ability to imitate is automatic and pervasive. It facilitates empathy, social interaction, and likeability (Iacoboni 2009). Non-human primates are also capable of imitating specific actions observed of a conspecific, such as a marmoset replicating an unusual way of opening a jar after observing a previously trained conspecific (Voelkl and Huber 2007). On top of that, they also have empathy, as evidenced by the fact that they can adopt the affective state of another individual (Meyza, Bartal et al. 2017), and that rhesus monkeys act altruistically in situations where they have to forego food rewards in a food deprived state to prevent a conspecific from getting shocked (Masserman, Wechkin et al. 1964).

Chimpanzees are also capable of social learning in nature and captivity, and will collaborate with their peers to acquire rewards (Hirata 2009). While these behaviours are potentially supported by several systems in the brain, it can be argued that the neural antecedents of these social processes peaked with the discovery of mirror neurons (Iacoboni 2009).

1.1 Motor Cortex and Mirror Neurons

The premotor area (Brodmann area F5) in monkey frontal cortex is associated with goal directed actions, conditional action learning and action preparation (Wise 1985, Iacoboni 2009). Strikingly, neurophysiological recording experiments in the 1990s documented that subsets of neurons in premotor cortex were activated by both the action of an animal as well as the mere observation of the same action performed by another individual (di Pellegrino, Fadiga et al. 1992). These cells were called “mirror neurons”, and have been characterized in the monkey premotor and posterior parietal cortices (Gallese, Fadiga et al. 1996, Rizzolatti, Fadiga et al. 1996, Rizzolatti and Luppino 2001, Iacoboni 2009). It has been hypothesized that mirror neurons can be useful for the survival of a species in different ways, such as action

recognition or empathy. They can be a powerful tool for understanding the actions and intentions of others and thus would facilitate social cognition (Iacoboni 2009).

Over the decades, studies have shown that mirror neurons in monkey premotor cortex respond to more than the pure motor execution aspects of behaviour and exhibit several properties which could facilitate "action understanding". For example, they have been shown to respond to the goals of specific actions differentially, such as grasping an object to eat or grasping an object to place it in a container (Fogassi, Ferrari et al. 2005), or to the use of normal or reverse-pliers (that require opening the hand) in order to grasp an object (Umiltà, Escola et al. 2008). In addition to encoding action goals, they can respond to similar actions that complement each other (di Pellegrino, Fadiga et al. 1992), and respond to stimuli in auditory as well as visual modalities (Iacoboni 2009). Evidence also suggests the existence of mirror neurons in the monkey premotor cortex that fire for facial expressions of a conspecific, including those both associated with ingesting and those that are associated with communication (Ferrari, Gallese et al. 2003). Together, these findings suggest that premotor mirror neuron activity is involved in coherent representations of observed actions and their goals (Iacoboni 2009).

Functional magnetic resonance imaging and transcranial magnetic stimulation studies suggest that the human brain also has mirror neurons and in regions homologous to the monkey premotor cortex (Gallese, Keysers et al. 2004, Rizzolatti and Fabbri-Destro 2008, Iacoboni 2009). In humans, suspected mirror neuron activity is believed to indicate social cognition and empathy (Pfeifer, Iacoboni et al. 2008) and, in support of this theory, children with autism have less activation in the equivalent areas when looking at human faces expressing major emotions (Dapretto, Davies et al. 2006, Iacoboni and Dapretto 2006).

1.2 Rodent Models of Social Cognition

In order to understand what role mirror neurons might play mechanistically in empathy or imitation in humans, it is intuitive that studies in human and non-human primates would be most relevant because of evolutionary proximity. However, studies in humans and monkeys have great limitations, such as ethical concerns, the cost of research and behavioural problems. From a methodological standpoint, rodents provide more accessible research models. They are more affordable to acquire, easier to breed in specific strains to minimize genetic variability and can be housed humanely in larger numbers. In terms of neural recordings, chronically implanted rodents can be trained to carry implants without problems, and genetic manipulation is far easier in rodent genomes.

Rodents have also proven fruitful models for studying social cognition, as they are capable of observational learning and empathy (Zohar and Terkel 1991, Knapska, Mikosz et al. 2010). Observational fear learning is a commonly explored phenomenon in rodents because it is easy to induce and typically yields robust results (Meyza, Bartal et al. 2017).

However, rodents also show prosocial altruistic behaviour, similar to non-human primates. Specifically, rats have been shown to prefer freeing a restrained conspecific instead of obtaining a highly valued food reward, and will then choose to share food with freed individual (Bartal, Decety et al. 2011). Rats would also alter their behaviour such as lever pressing to relieve a conspecific from getting shocked (Meyza, Bartal et al. 2017). In mice, it has been shown that animals who observed a conspecific receive shocks will interact with the shocked animal more after the observation of fear conditioning (Allsop, Wichmann et al. 2018).

In light of these and other results, it is reasonable to investigate social cognition in rodents in terms of neural mechanisms, including mirror neuron-like neural activity or general neural representations of social interaction.

Even though rodents lack an exact homologue of the primate premotor cortex, they have a frontal motor area which is distinct from primary motor cortex (M1). Previous anatomical, physiological and behavioural work has revealed many architectural and functional properties which suggest that secondary motor cortex (M2) in the rodent brain has similar characteristics to the monkey frontal eye fields, premotor, and supplementary motor areas (Deffeyes, Touvykine et al. 2015, Barthas and Kwan 2017), thus making M2 a likely target for investigating mirror neuron-like activity.

Anterior cingulate cortex (ACC) is another significant area for social cognition, empathy and theory of mind. Human imaging studies associate ACC with development of joint attention and theory of mind, which are essential for human socialization and empathy (Iacoboni 2009). The inputs to ACC from many structures including sensory areas and association cortices make it a reasonable area to inspect for mechanisms of social cognition (Fillinger, Yalcin et al. 2017).

Social cognition paradigms typically rely heavily on the observation of a conspecific—either through vision or audition. However, tactile information is also important for rodents in social contexts (Bobrov, Wolfe et al. 2014), and social touch in rodents has been shown to facilitate social buffering of aversive stimuli (Meyza, Bartal et al. 2017).

For example, a behavioural study in rats found that physical contact with a familiar cage mate after social defeat prevented increased anxiety in an elevated maze task carried out two weeks later (Nakayasu and Kato 2011). Control experiments then showed that cage mates housed with a wire mesh separator allowing visual, auditory and olfactory inputs, but impairing free tactile interaction, abolished this effect, with the subjects showing similar anxiety to control animals housed alone (Nakayasu and Kato 2011).

Therefore, the representation of social interactions in rodent brain might not be restricted to visual or auditory observation, and it is worthwhile to explore how tactile interactions might drive social representations in relevant brain regions.

1.3 Secondary Motor Cortex

1.3.1 Anatomy of the Secondary Motor Cortex

Secondary motor cortex is a prominent structure in the rodent frontal cortex, and is associated with a myriad of functions including action selection and motor learning (Barthas and Kwan 2017). The nomenclature previously adopted reflects suspected functions of this area, such as involvement in orienting movements of the head (Erlich, Bialek et al. 2011) and whisker movements (Hill, Curtis et al. 2011). Accordingly, some of the labels used include vibrissae motor cortex, frontal eye field (FEF) or frontal orienting field (FOF), agranular medial area (AgM) (Brecht 2011).

However, the area has a different connectivity pattern compared to M1, and each area has distinguishing cytoarchitecture and laminar morphology (Barthas and Kwan 2017, Ebbesen, Insanally et al. 2018). In this study, the area termed secondary motor cortex (M2) will be defined according to the ongoing research from the Whitlock Lab at the Kavli Institute for Systems Neuroscience (Mimica, Dunn et al. 2018, Hovde, Gianatti et al. 2019, Olsen, Hovde et al. 2019, Tombaz, Dunn et al. 2019) and previous M2 literature (Sul, Jo et al. 2011, Cao, Ye et al. 2015, Yamawaki, Radulovic et al. 2016, Barthas and Kwan 2017).

In the rodent brain, M2 appears in frontal cortex along the midline of the brain, and is bordered caudally by posterior parietal cortex (PPC). M2 runs medial to primary motor cortex (M1) and dorsolateral to the dorsal anterior cingulate cortex (dACC) (Figure 1). In this study, M2 is delineated according to the Paxinos and Franklin Mouse Brain Atlas (2012) and previous literature (Sul, Jo et al. 2011, Cao, Ye et al. 2015, Yamawaki, Radulovic et al. 2016, Barthas and Kwan 2017).

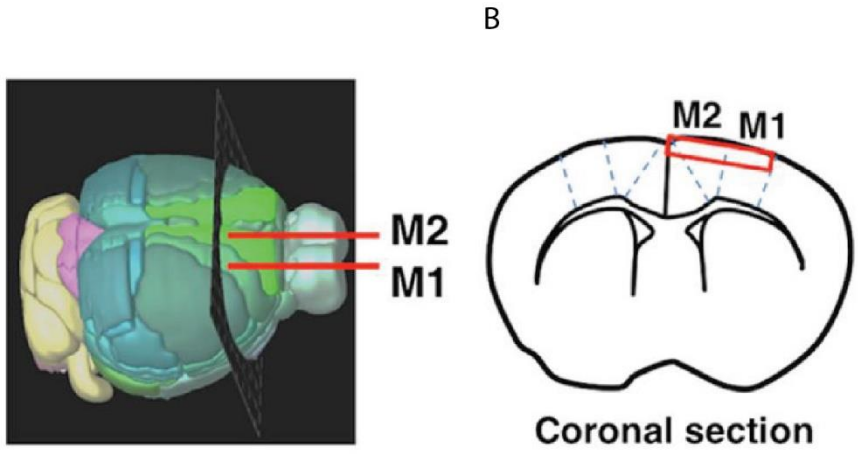

Figure 1 Anatomy of the secondary motor cortex (M2)

A. Anatomy of the secondary motor cortex. **B.** Coronal section at the level of black plane on A.

Figure adapted from (Cao, Ye et al. 2015).

1.3.2 Connectivity of Secondary Motor Cortex

M2 is defined by reciprocal connections with many cortical and thalamic structures. Connections with cortical structures include visual cortex, posterior parietal cortex (PPC), anterior cingulate cortex, retrosplenial cortex (RSC), and orbitofrontal areas (Reep, Goodwin et al. 1990, Zingg, Hintiryan et al. 2014).

Unlike primary motor cortex (M1), M2 has strong connections with different subdivisions of PPC. Medial PPC projections are targeted to caudal parts of M2 (caudal to and around Bregma), whereas lateral PPC and the caudolatetal subdivision of PPC (PtP) project most densely to intermediate M2 (caudal to the genu of the corpus callosum, but rostral to Bregma (Olsen, Hovde et al. 2019).

M2 also receives input from visual cortex projections (Mohajerani, Chan et al. 2013), with visual areas 17, 18 and 18a projecting to the most caudal part of M2 (Miller and Vogt 1984). A later study found reciprocal connections between areas of M2 rostral to Bregma and higher visual areas (Itokazu, Hasegawa et al. 2018), while across studies primary visual cortex has been found to have weaker connections to M2.

As for frontal connections with neighbouring frontal areas, M2 projects to both dorsal and ventral anterior cingulate cortex (Zingg, Hintiryan et al. 2014, Fillinger, Yalcin et al. 2017). It also has reciprocal connections with several subdivisions of the orbitofrontal cortices (Olsen, Hovde et al. 2019).

M2 and RSC also have reciprocal connections, and it has been observed that subsets of RSC neurons appear to generate a RSC-PPC-M2 disynaptic circuit (Yamawaki, Radulovic et al. 2016). (Refer to Figure 2 for a schematic network including M2 connections)

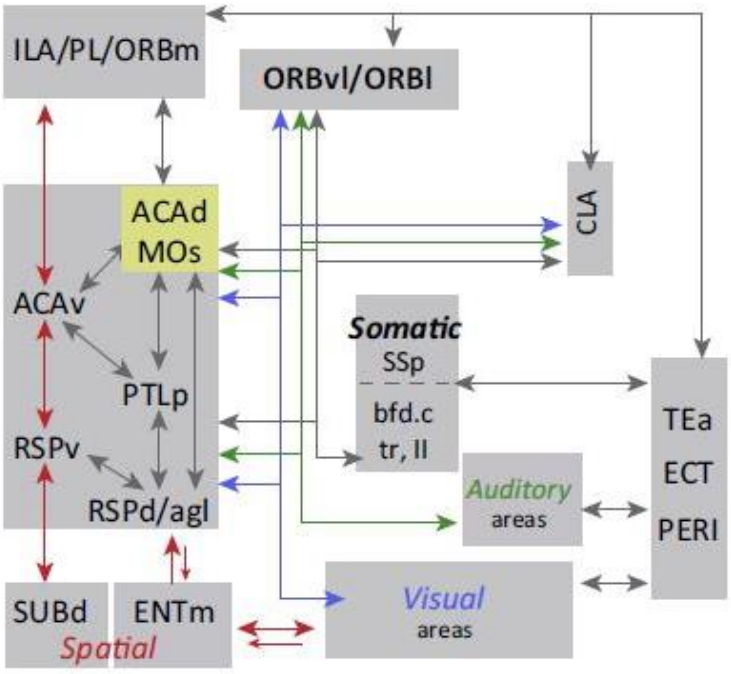

Figure 2 Overview of medial network interactions including M2 and ACC

Connectivity of M2 (referred as MOs here) and ACC (referred as ACAd and ACAv here) with association and primary sensory cortices.

See abbreviation list for areas.

Figure adapted from (Zingg, Hintiryan et al. 2014, Barthas and Kwan, 2017).

1.3.3 Functions of Secondary Motor Cortex

Frontal Motor Areas in Rodents?

In addition to the anatomical parallels between rodents and primates, which include prominent input from PPC as well as connections with prefrontal areas and descending motor efferents, there are also functional similarities across species. Microstimulation of anterior portions of M2 in mice, for example, elicits eye shifts in mice (Itokazu, Hasegawa et al. 2018), which is similar to the frontal eye fields in macaques (Barthas and Kwan 2017, Ebbesen, Insanally et al. 2018). Mice can also be trained to make voluntary eye movements on cue, similar to saccadic eye movements in primates, which are impaired during optogenetic suppression of M2 but not M1, and calcium imaging of this area shows activation just before the onset of eye movements (Itokazu, Hasegawa et al. 2018). These findings support that M2 has functional parallels to frontal eye fields in the monkey (Robinson and Fuchs 1969, Bruce and Goldberg 1985) and human brain (Paus 1996) which are important for online behaviour and, in addition, are considered important for social interaction. Dysfunctional frontal eye fields in humans, for example, can be associated with disturbances with eye movements in autism spectrum disorder (Mundy 2003).

It has also been shown that some neurons in M2 modulate their activity based on action selection in a free choice task (Sul, Jo et al. 2011), with cells starting to show changes in activity approximately 500 ms before the onset of chosen actions in a T-maze. Furthermore, population activity in M2 could be used to decode the chosen action. Some neurons responded after the fact for specific actions, reaching the reward or the interaction of the two with low but persistent activity. It was interpreted that this activity affected the next action choice of the animal (Sul, Jo et al. 2011).

A study using a waiting task, in which rats could choose to wait for two cues for a large reward or one cue for a small reward, suggest that some neurons in M2 are associated with voluntary action initiation (Murakami, Vicente et al. 2014). It was found that one class of neurons increased their firing rate up to a certain threshold until just before the initiation of movement (Murakami, Vicente et al. 2014). This kind of neuronal activity in other tasks, such as sensory decision making can also be associated with primate premotor cortex (Ebbesen, Insanally et al. 2018).

Actions in Context

It has also been argued that M2 activity is associated with motor learning rather than motor execution (Barthas and Kwan 2017), and that M2 is specifically important when an animal needs to learn something new or adapt to the environment. For example, a motor learning task requiring walking on a rotating rod with skilled steps activates and consolidates neuronal ensembles in M2 while the animals improve during training (Cao, Ye et al. 2015). Moreover, lesion and inhibition studies of M2 did not report impaired behaviour in response to direct motor commands (Barthas and Kwan 2017), however, M2 inactivation led to deterioration of

movement adaptation to reward probabilities with regard to prior action outcomes (Sul, Jo et al. 2011, Barthas and Kwan 2017). This activation was also specific to relevant behaviors for a learned task and modulated by conditional rules. Inactivation of M2 leads to persistent errors in cue guided actions, and if the task is switched to non-cued responses the number of errors is reduced (Barthas and Kwan 2017).

Social Cognition

A recent study specifically investigated whether M2 expressed neural correlates for observed motor actions, but did not reveal mirror neuron activity (Tombaz, Dunn et al. 2019). This lack of apparent tuning might not be absolute, however, as another social cognition study suggested the existence of affective mirror neuron activity in the rat anterior cingulate cortex (ACC), which also had recording cites in M2 (Carrillo, Han et al. 2019). Specifically, that work showed that rat brain had affective mirror neurons that respond to self-pain and pain experienced by a conspecific in an observational fear learning paradigm. M2 is also involved in whisker movement, which provides essential sensory input for rodents during an array of natural behaviors, including exploration, locating object and social interactions (Barthas and Kwan 2017, Ebbesen, Insanally et al. 2018). Thus, representation of a conspecific in M2 might not be confined to only visual information, and tactile information from social interactions (Bobrov, Wolfe et al. 2014), which are strongly encoded in somatosensory cortex, could be important for the neural representation of social interaction in M2.

1.4 Anterior Cingulate Cortex (ACC)

1.4.1 Anatomy of the Anterior Cingulate Cortex

The ACC is a brain region associated with a myriad of functions including emotional processing, cognitive functions and pain cognition (Fillinger, Yalcin et al. 2017). Across mammalian species, this area was defined in early literature as cingulate cortex, a large structure that curves around corpus callosum which constitutes a part of the limbic system involved in emotion processing. Various studies revealed that, in the human and primate brain, cingulate areas are heterogeneous in function (including emotion processing, pain cognition, and attention) and cytoarchitecture (Vogt, Finch et al. 1992). The heterogeneous nature of the area, as reflected by differences in cytoarchitecture, imaging results, and receptor makeup shaped the borders and nomenclature of the cingulate cortex. The structure is accordingly divided into anterior cingulate (ACC), midcingulate (MCC) and posterior cingulate (PCC) cortical subdivisions (Vogt, Finch et al. 1992).

Historically, in the rodent brain, the anterior cingulate cortex (consisting of Cg1 dorsally and Cg2 ventrally) was defined as a large structure in the dorsal part of the medial prefrontal cortex (Fillinger, Yalcin et al. 2017). Though the subdivisions of the ACC are contiguous, the rodent cingulate cortex is not homogeneous in structure or function. As more evidence accumulated from functional and neuroanatomical studies, the ACC and MCC were introduced as different areas in the rodent brain (Vogt and Paxinos 2014), which provided a better and clearer point of comparison across human, monkey and rodent brains (Figure 3) (Vogt, Hof et al. 2013, Vogt and Paxinos 2014). In rats and mice, the ACC comprises areas 24a (ventral ACC) and 24b (dorsal ACC), while MCC consists of 24a' (ventral MCC) and 24b' (dorsal MCC) (Vogt and Paxinos 2014, Vogt 2015, Fillinger, Yalcin et al. 2017).

Cingulate cortex as a whole lies dorsomedial to corpus callosum, along the midline of the rodent forebrain. Dorsal ACC starts around the anterior forceps and is joined by ventral ACC around the genu of the corpus callosum. The structures extend caudally until around Bregma, where they are bordered by MCC, which is itself bordered caudally by retrosplenial cortex (Vogt and Paxinos 2014, Fillinger, Yalcin et al. 2017).

For this study, ACC borders labelled as Cg1 (dorsal ACC) and Cg2 (ventral ACC) are in accordance with the Paxinos and Franklin Mouse Brain Atlas (2012). Further divisions between ACC and MCC will be defined according to previous neuroanatomy studies from Vogt and Paxinos (2014) and Fillinger et al. (2017). Finally, to keep the size of the analysis manageable for the time available to the project, the study focused on ACC between Bregma levels +1.0 and +0.5. From here on, dorsal ACC (dACC) and ventral ACC (vACC) will be used to refer to areas 24b and 24a, respectively (Figure 3). ACC will be used to refer to both dACC and vACC, together.

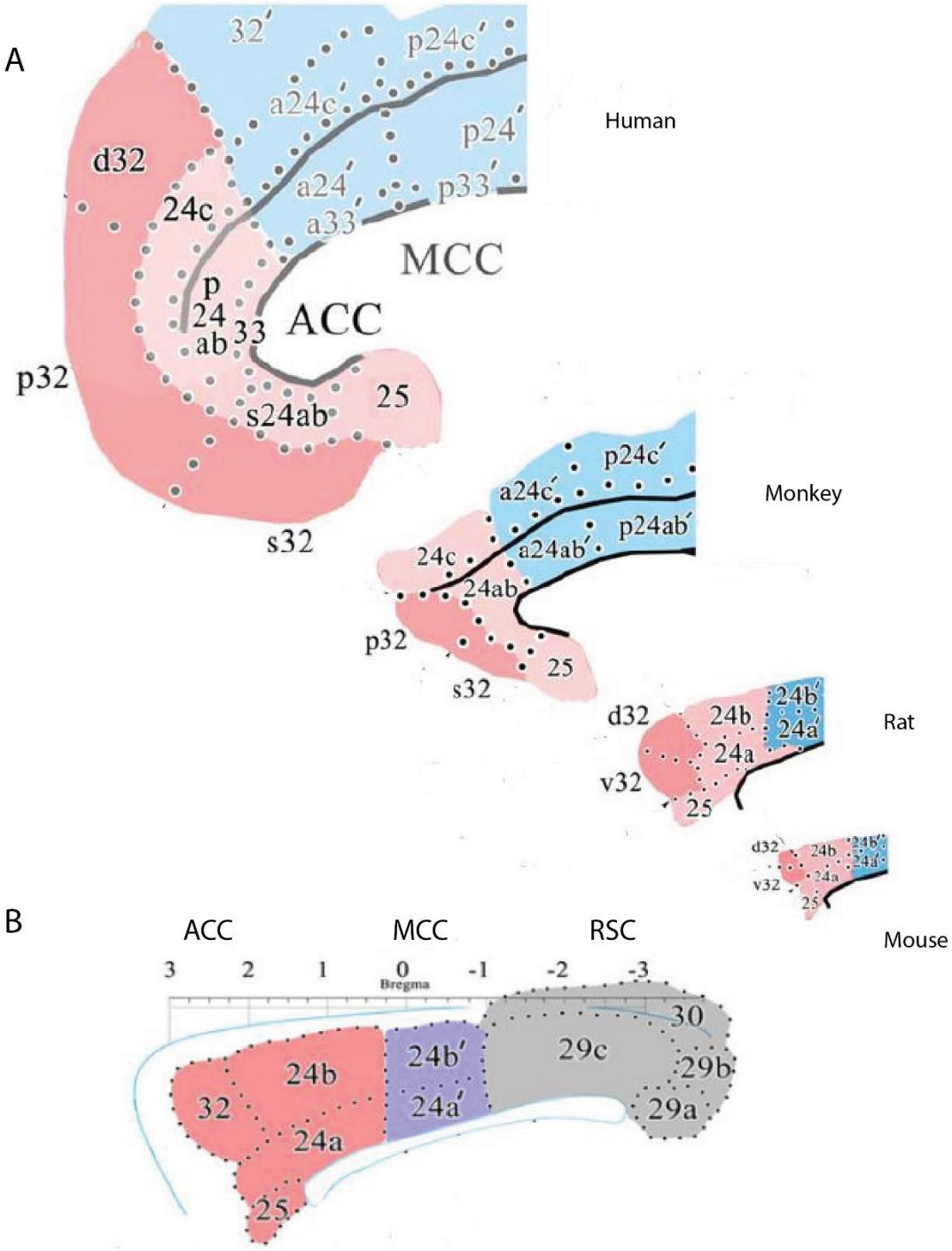

Figure 3 Anatomy of mouse ACC with rat, monkey and human homologies

A. Flat maps of human, monkey, rat and mouse ACC (24a/b) and MCC (24a'/b') **B.** Flat map of mouse ACC, MCC and RSC. 24a refers to vACC, 24b refers to dACC.

Figure adapted from Vogt, Hof et al. 2013, Vogt and Paxinos 2014.

1.4.2 Connectivity of Anterior Cingulate Cortex

As a substantially sizeable polymodal cortical area, ACC has many reciprocal or otherwise unilateral connections with many brain regions. These include intracingulate connections across cingulate structures, connections with other cortical structures (discussed below), various thalamic nuclei, the basal forebrain, as well as primarily monoaminergic centres of the brainstem and hypothalamus (Vogt 2015, Fillinger, Yalcin et al. 2017). Here, only connectivity of the ACC in the rodent brain relevant to the topic will be discussed.

The ACC has dense connections with structures in medial prefrontal cortex, including strong connections with secondary motor cortex (M2) (Vogt 2015, Barthas and Kwan 2017, Fillinger, Yalcin et al. 2017), and reciprocal connections with retrosplenial cortex (RSC) (areas 29 and 30). Connections with dACC are denser than those with vACC (Vogt and Miller 1983, Fillinger, Yalcin et al. 2017). The ACC also has connections with primary sensory areas including somatosensory, visual, and auditory cortices and with associational areas such as the PPC (Vogt and Miller 1983, Mohajerani, Chan et al. 2013, Fillinger, Yalcin et al. 2017, Hovde, Gianatti et al. 2019). dACC has denser connections with visual cortex than vACC (Vogt and Miller 1983).

There is also evidence that dACC shows functional coupling with some of these areas, indicated by synchronous neural activation with PPC, primary somatosensory and primary visual cortices during different phases of a tactile stimulus discrimination task (Kunicki, R et al. 2019). Interestingly, the same study also indicated information flow between ACC and these same areas (Kunicki, R et al. 2019).

Subcortically, tracer labelling has shown the existence of strong connections between the claustrum and the ACC and, again, dACC connections were denser compared to vACC (Fillinger, Yalcin et al. 2017). The ACC also has connections with anterior basolateral nucleus of amygdala (BLA), a projection implicated specifically in the acquisition of vicarious fear of conditioned stimuli (Fillinger, Yalcin et al. 2017, Allsop, Wichmann et al. 2018).

Considering the strong connections with PPC and the claustrum, ACC receives highly processed sensorimotor information which epitomizes the ACC's role as an association area (Figure 2 and 4) (Fillinger, Yalcin et al. 2017).

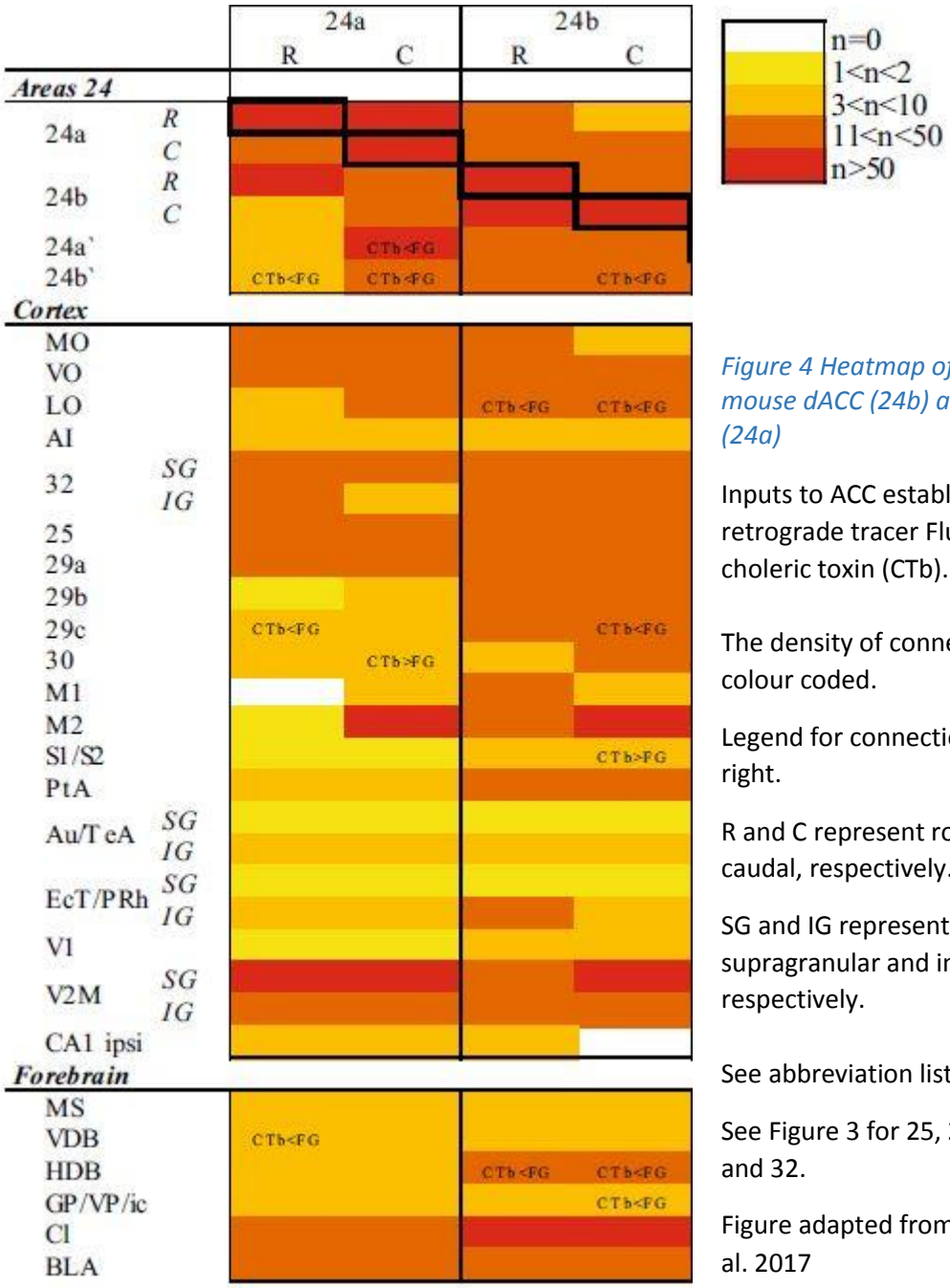

Figure 4 Heatmap of afferents to mouse dACC (24b) and vACC (24a)

Inputs to ACC established by retrograde tracer FluoroGold and choleric toxin (CTb).

The density of connections are colour coded.

Legend for connections is at top right.

R and C represent rostral and caudal, respectively.

SG and IG represent supragranular and infragranular, respectively.

See abbreviation list for areas.

See Figure 3 for 25, 29a/b/c, 30 and 32.

Figure adapted from Fillinger et al. 2017

1.4.3 Functions of Anterior Cingulate Cortex

As an association area with extensive connections with other cortical and subcortical structures, the ACC is involved in a plethora of processes. These processes range from coordinate transformations for motor control to different types of cognitive and emotional regulation (Devinsky, Morrel et al. 1995, Bush, Luu et al. 2000).

For the present study, the most important functions implicated in the ACC literature include social cognition, empathy, social and observational learning.

Previous research suggests that the ACC is involved in social cognition and emotion processing in humans, monkeys and rodents, and those functions will be considered below.

Social Cognition, Emotion Regulation, and Observational Learning in ACC

Human and Monkey Studies

As mentioned above, previous literature on the ACC adopts a variety of borders and nomenclature. Thus, dorsal or ventral AAC divisions in human and monkeys do not always correspond to the same areas in the rodent brain. Here, the brain regions from human and monkey research that are thought to be equivalent to rodent brain areas 24a and 24b were referred as the ACC.

In monkeys, lesioning the ACC disrupts the mother-infant relationship, such that the separation cry of the infant and attentiveness of the mother are impaired (Devinsky, Morrel et al. 1995).

In macaques, the ACC is also important for social interest in conspecifics. Male macaque monkeys are interested in looking at images of either a higher ranking male or sexually presenting female, and they would refrain from retrieving food or do so more slowly in favour of these images (Rudeback, Buckley et al. 2006). Animals with ACC lesions, on the other hand, were not interested in social stimuli and were quicker to retrieve food than normal animals or cohorts who received sham lesions. However, the lesions did not affect their reaction to a fear inducing stimulus (a moving toy snake) (Rudeback, Buckley et al. 2006).

Another function which has ACC involvement is theory of mind (ToM). ToM is a developmental hallmark that is fundamental for human socialization, and refers to the ability to differentiate the mental states of the self from mental states of others. These mental states can include emotions and intentions, among many other cognitive attributes. Children on the autism spectrum, for example, score lower on verbal and non-verbal ToM tasks which are associated with overlapping areas of dorsomedial prefrontal cortex and the ACC. Functional studies using positron emission tomography (PET) and magnetic resonance imaging (MRI) also suggest that people with autism and Asperger's disorder show a volumetrically smaller ACC and lower metabolic activity in ACC (Mundy 2003). In terms of social anxiety, a recent MRI study found that people with generalized anxiety disorder, generalized social phobia or both had reduced

dACC activity, while healthy controls had elevated activation levels during emotion regulation tasks involving affective cues (Blair, Geraci et al. 2012).

Additional functional investigations in healthy human subjects have provided further evidence supporting a role for the ACC in social cognition, including work showing a specific role for the ACC in processing emotive facial expressions (Devinsky, Morrel et al. 1995). A separate study also showed that ACC activation in humans was associated with tracking self-mental states or attributing mental states to others, while activation of other parts of ACC was associated with the observation of freely moving conspecifics (Frith and Frith 2001).

A meta-analysis of human functional MRI studies associated ACC activation with social pain in the form of social rejection and exclusion (Rotge, Lemogne et al. 2015). This activation was greater in children than in adults, suggesting a developmental aspect of processing social cues (Rotge, Lemogne et al. 2015). Interestingly, Somerville et al. found that human ACC has increased activation in social validation during a social acceptance feedback task (Somerville, Heatherton et al. 2006). These results also support the idea that ACC has an important role in top down emotion regulation and processing. Previous literature also suggests that activity in ACC can be negatively correlated with activity in amygdala during the processing of negative affective stimuli, while parts of ACC are activated by positive affective stimuli (Etkin, Egner et al. 2011).

Rodent Studies

In mice, multiple lines of work suggest that the ACC plays a fundamental role in social pain processing. In one such study, an alcohol withdrawal experiment was performed in which alcohol-naïve bystander mice that were housed and tested in the same room with cohort animals undergoing alcohol withdrawal developed similar hyperalgesia as tested by a mechanical sensitivity threshold. Control mice that were housed and tested in a separate room did not develop hyperalgesia. Both bystander and experimental animals showed elevated *c-Fos* activity in dACC compared to controls, and chemogenetic inactivation of dACC by DREADD abolished the hyperalgesia in bystander mice (Smith, Walcott et al. 2017).

A more recent study in rats provided evidence that the ACC responds to the affective properties of pain experienced by a conspecific (Carrillo, Han et al. 2019). In this study, observer rats that had experienced painful laser stimulation on the foot showed mirror neuron-like activity in ACC while observing a conspecific receive foot shocks. That is, these “emotional mirror neurons” were activated by both self-experienced pain and observed pain, but not for a conditioned stimulus alone. On the other hand, there were cells that were active for the observed pain and the conditioned stimulus, which were named “fear mirror neurons” (Carrillo, Han et al. 2019).

In line with these observations, ACC was also shown to play a critical role in observational fear conditioning in rodents (Allsop, Wichmann et al. 2018). Specifically, it was found that the

connection between the ACC and basolateral amygdala (BLA) were important for vicarious fear acquisition, as optogenetic inhibition of ACC→BLA projections was shown to eliminate observational fear conditioning, but did not affect classical fear conditioning. This inhibition also diminished social interaction with a novel juvenile conspecific introduced to the home cage, but not exploration of novel objects. During observational fear conditioning, observer mice mimicked the escape behaviour of the demonstrator mice, and inactivation of the ACC to BLA projections also decreased the mimicking behaviour of the observers. Inhibition or stimulation of the pathway did not have an effect on locomotion or behaviour related to anxiety, suggesting the pathway is important for social cues regardless of their anxiogenic or anxiolytic properties (Allsop, Wichmann et al. 2018).

As mentioned previously, the ACC receives visual inputs that are important for observational fear learning (Allsop, Wichmann et al. 2018), and it also modulates other cortical areas during tactile discrimination task in rodents (Kunicki, R et al. 2019). Though the ACC processes these different sensory inputs and modalities as well as different forms of social behaviour, it is still not known whether the same or different neural ensembles within the ACC respond differentially to a conspecific by vision or touch.

1.5 Cellular Compartment Analysis of Temporal Activity by Fluorescent in Situ Hybridization (catFISH)

1.5.1 Immediate Early Genes

Immediate early genes (IEGs) are genes that are transcribed immediately after neuronal activation, and can be induced in response to a multitude of stimuli (Davis, Bozon et al. 2003). IEGs are, by definition, transcribed by pre-existing transcription factors in the cell and do not require new protein synthesis, which allows rapid transcription that can be initiated in an instant (Okuno 2011).

Approximately 40 IEGs have been identified to date (Davis, Bozon et al. 2003). These IEGs encode a plethora of proteins, however, their functions can be roughly divided in two. IEG products can themselves be transcription factors that regulate downstream gene expression, such as with the *Fos* related proteins *c-Fos* and *zif268*, while other IEG products such as *Arc*, *Homer1a* and *Narp,* are proteins directly involved in cytosolic and synaptic activities (Davis, Bozon et al. 2003, Okuno 2011).

Their widespread occurrence across brain regions and rapid activation make IEGs perfect markers for recent neural activity, and their activation be detected in brain tissue using immunohistochemistry against their protein products, or against their mRNA using in situ hybridization (ISH) (see Methods.3 for ISH description).

1.5.2 Immediate Early Gene *Arc* (Activity Regulated Cytoskeleton Protein)

In terms of identifying recently active neurons, the IEG *Arc* has several advantages over other IEGs, such as *zif268* or *c-Fos*. First, it has been shown that *Arc* is involved in synaptic plasticity by mediating AMPA receptor scaling (Shepherd, Rumbaugh et al. 2006), *Arc* protein inhibition leads to impairments of long term potentiation and memory consolidation (Guzowski, Lyford et al. 2000). In line with these functions, *Arc* expression is induced by a variety of tasks and stimuli including novel environment exploration, spatial memory tasks, olfactory memory tasks and operant learning tasks (Guzowski, McNaughton et al. 1999, Okuno 2011).

Activity-dependent expression of Arc IEGs in the brain has been observed in regions including, but not limited to, the hippocampus, entorhinal cortex, striatum, amygdala and various cortical regions (Guzowski, McNaughton et al. 2001). Hippocampal *Arc* expression was correlated with the learning of a spatial (hippocampus dependent) task but not with a cued (non-hippocampus dependent) task while *c-Fos* and *zif268* activation levels were similar for both tasks (Guzowski, Setlow et al. 2001).

In terms of intracellular spatial confinement, *Arc* mRNA is more localized than *c-Fos* and *zif268*, as it is swiftly translocated to the dendrites following transcription, which produces lower background somatic staining (Guzowski, Setlow et al. 2001). *Arc* mRNA transcription also has specific temporal characteristics concerning transcription latency and translocation to the cytoplasm which allows *Arc* expression to disambiguate two temporally isolated events (Guzowski, McNaughton et al. 1999, Guzowski, McNaughton et al. 2001).

1.5.3 CatFISH

The time course of *Arc* signal and its distribution can be assessed via cellular compartment analysis of fluorescence in situ hybridization, or “catFISH”. This approach exploits the fact that *Arc* mRNA accumulates in the cell nucleus within two minutes of induction and will stay for up to 15 minutes, which effectively produces an intranuclear RNA signal for cellular activity within 15 minutes of stimulus removal. After 15 minutes, Arc mRNA is translocated to the cytoplasm where it can be detected 20 to 45 minutes post-induction, while intranuclear mRNA signal returns to baseline levels within 30 minutes (Guzowski, McNaughton et al. 1999, Guzowski, McNaughton et al. 2001).

The distinct latency characteristics of intranuclear and cytoplasmic *Arc* signal act as a powerful tool to evaluate the activation patterns of the same neurons at two different time points or epochs that are 20 minutes apart (Guzowski, McNaughton et al. 1999, Guzowski, McNaughton et al. 2001).

In past studies using catFISH (e.g. Vazdarjanova and Guzowski 2004, Burke, Chawla et al. 2005), neural activation during two different 5-minute epochs of behaviour was distinguished by quantifying the nuclear or cytoplasmic localization of *Arc* signal. The epochs were divided by a 20-minute delay period where animals were placed in their home cage, undisturbed.

If a cell is active only in the first 5-minute epoch of the behaviour or task, *Arc* signal will be only cytoplasmic. If the cell is active only in the second 5-minute epoch, the *Arc* signal will be only in the nucleus. However, *Arc* mRNA will be visible in both the nucleus and the cytoplasm if the cell is active during both epochs (Figure 5) (Guzowski, McNaughton et al. 1999, Guzowski, McNaughton et al. 2001, Burke, Chawla et al. 2005). Furthermore, since *Arc* expression is elevated by novel stimuli and does not occur under basal behavioural conditions, control animals are typically left undisturbed in their home cages to allow comparisons of baseline activity (Guzowski, McNaughton et al. 1999, Guzowski, McNaughton et al. 2001, Vazdarjanova and Guzowski 2004, Burke, Chawla et al. 2005, Burke and Barnes 2015).

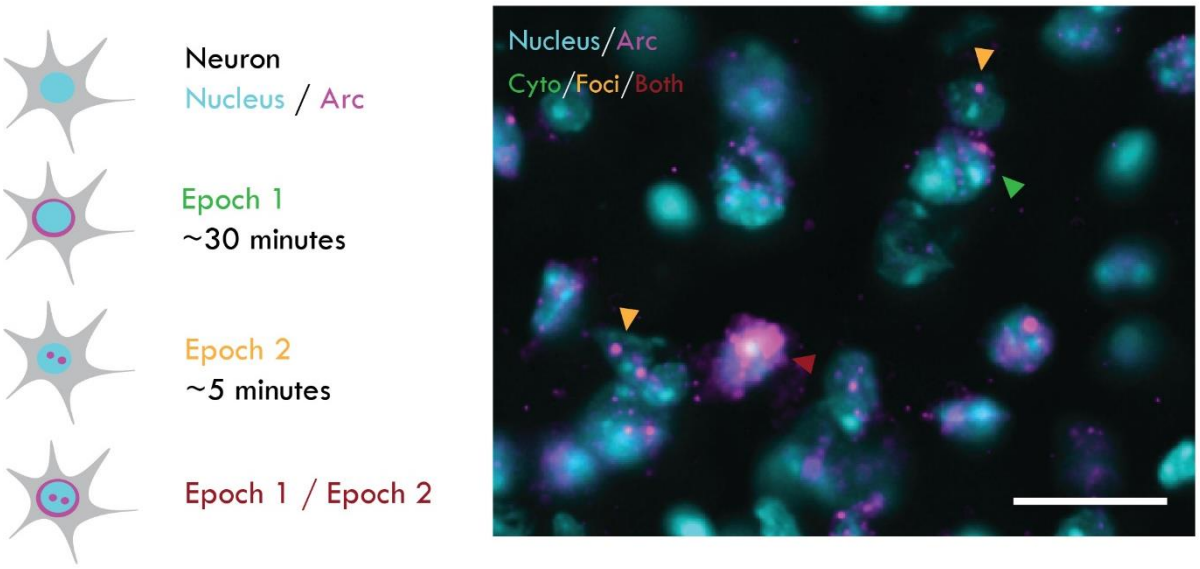

Figure 5 Intracellular Arc localization disambiguates neural activation across epochs

Left, Schematic of *Arc* signal localization during distinct behavioural epochs. If a cell is only active during epoch 1, the signal will be only cytoplasmic. If the cell is only active during epoch 2, the signal will be only in the nucleus. The cells which are active during both epochs will have both intranuclear and cytoplasmic signal. Right, Small portion of a z-stack, with orange arrows marking intranuclear signal, a green arrow marking cytoplasmic signal, and a red arrow indicating both intranuclear and cytoplasmic signal. Scale bar = 25µm.

The catFISH method reports neural activity retrospectively and does not require injections or pre alterations. The data are collected post factum via in situ hybridization of mRNA, and this retrospective nature brings forth several caveats and advantages. One drawback is that, even though catFISH is used to distinguish two temporally distinct epochs of behaviour, the method cannot provide a precise temporal readout of neural activity during behaviour. On the other hand, catFISH allows for impeccable control over the brain area investigated because the image collection for analysis is done after the brain area is detected and delineated. Animal behaviour is not affected by any kind of tethers or head implants and, because the method does not require surgery, the animals are spared any post-operative stress or physiological strain.

1.6 Aim

Previous studies have shown that rodents are capable of empathy and social learning. However, how distinct social experiences are represented at the cellular level in rodent brain is not clear. M2 and ACC are two associative frontal areas that receive sensory input both from other association areas and primary sensory cortices, and have to varying degrees been implicated in social cognition in several mammalian species. Thus, both areas are reasonable targets to study the cellular correlates of social cognition. While it was recently found that M2 in mice did not show mirror neuron like activity for observed actions (Tombaz et al., 2019), the ACC was shown to exhibit affective mirroring in response to observational fear learning in rats (Carrillo et al. 2019).

The present study aims to add to this knowledge by exploring whether cell populations in M2 and AAC in mice are activated differentially in social contexts which are limited to visual input, or which also allow physical interactions between animals. Tactile interaction is an ethologically fundamental, natural behaviour in rodents which can be a strong contributor to empathy. The secondary aims of the study is to explore social cognition in mice in the context of positive social interaction without components of pain and fear which has been neglected in the previous rodent ACC literature.

To disambiguate how M2 and ACC respond to visual and tactile information from the same conspecific, we will investigate neural responses in these areas following behavioural episodes allowing direct physical interaction, or during visual observation sessions in which animals are separated by a transparent barrier. *Arc* catFISH will be used to identify which neural populations are activated by these different experiences while keeping animal behaviour as naturalistic as possible in a lab setting.

We hypothesize that tactile interaction with a conspecific will have a differentiated representation than observation of the same target. Therefore we expect Arc signal distribution in the investigated areas to reflect this hypothesis in the form of differentiated *Arc* labelling in cell ensembles across epochs (tactile interaction vs. observation).

Chapter 2

Methods and Materials

The reagent vendors and solution recipes can be found in Appendix A and B, respectively. FISH protocols can be found in Appendix C and list of software used can be found in Appendix D.

2.1 Behaviour and Animals

2.1.1 Animals

A total of nine male C57 mice were used for the experiments. Eight animals were provided by the Kavli Institute of Systems Neuroscience (Taconic). Six animals were used in experimental conditions and two served as naïve, cage-only controls. One male C57 mouse was given maximal electroconvulsive shock (MECS) as a positive control to ensure proper binding of the riboprobes; the animal was provided by and given MECS at the Burke Lab, McKnight Brain Institute, University of Florida (Table 1).

	Animal	Age	Sex	Condition
Pair 1*	Jagger	19w6d	M	Cage control
	Bowie		M	
Pair 2*	Damian	30w1d	M	Int - Obs
	Richard		M	
Pair 3	Jason		M	Obs - Int
	Timothy		M	
Pair 4	Johnny	27w	M	Obs - Int
	Cash		M	
Positive control	Gator	-	M	MECS tissue

Table 1 Animals and Conditions

The table lists all animals used in the project. Siblings and cage mates are highlighted with the same colour. The cages were separated prior to the handling phase.

The positive control animal was provided and handled by the McKnight Brain Institute, University of Florida staff.

All other animals were provided by the Kavli Institute for Systems Neuroscience, NTNU.

The data used in the analyses in the thesis came from animals marked with *.

The animals provided by the Kavli Institute were housed and handled in compliance with the institute's standards. Animals were kept on a reversed 12 hour day-night cycle and had free access to food and water.

2.1.2 Experimental Set-up

All eight animals were placed in separate cages at the beginning of the handling and habituation stage, and were handled once daily for eight days before habituation. The cage control animals were not included in the habituation step and were not exposed to the experimental chamber but had extra handling sessions two days prior to experiments. The remaining six animals were habituated to the experimental chamber for nine days.

A standard clear acrylic mouse cage (45cmX19.5cmX26cm) was modified to serve as the experimental chamber. Namely, the cage was wrapped with opaque material and a thin, non-perforated plastic sheet was attached securely in the middle with tape (Figure 6C) and a transparent lid was introduced to prevent animals from jumping out. Standard mouse bedding was used in the cage to allow the animals to move comfortably. The behavioural sessions were carried out on a raised platform which was closed off with opaque blue curtains, and the room was kept in dim light. The sessions were recorded via two high-speed, near-infrared cameras (Simi Reality Motion Systems GmbH, Germany).

Animals were paired off for each of the social interaction experiments. To decrease the possibility of fighting during the experiment, each pair consisted of siblings which were former cage mates.

For the experiments themselves, one pair completed a 5-minute “direct interaction” condition, separated by 20 minutes, then a 5-minute “observation through screen” sequence. Two pairs of animals also completed the counterbalanced order (Table 1).

The two pairs of animals in the counterbalanced condition fought during the “direct interaction” epoch, and were thus excluded from the analysis.

2.1.3 Behaviour Experiment Design

The two behavioural epochs investigated were “direct interaction (INT)” and “observation through a transparent separator (OBS)”. As noted above, the behavioural epochs lasted 5 minutes each and were divided by a 20 minute undisturbed home cage period.

At the start of each behavioural experiment, animals were placed in separate compartments of the experimental chamber.

For epoch 1 (INT), the separator was lifted immediately, allowing the animals to interact physically with each other freely for five minutes (Figure 6A).

After the first behavioural epoch, the animals were placed in their home cage for 20 minutes. The bedding was changed and the experimental chamber was wiped with 70% ethanol (Figure 6B).

For epoch 2 (OBS), animals were left to observe each other through the transparent separator for five minutes. The separator was non-perforated and securely attached to the cage, leaving no gaps (Figure 6C).

The duration of the behavioural epochs and the home cage period was determined according to the nature of *Arc* mRNA synthesis and translocation within the cell (Guzowski, McNaughton et al. 1999). *Arc* mRNA is transcribed within two minutes of neural activation, and the mRNA translocate to the cytoplasm 15-20 minutes after activation (Guzowski, McNaughton et al. 1999).

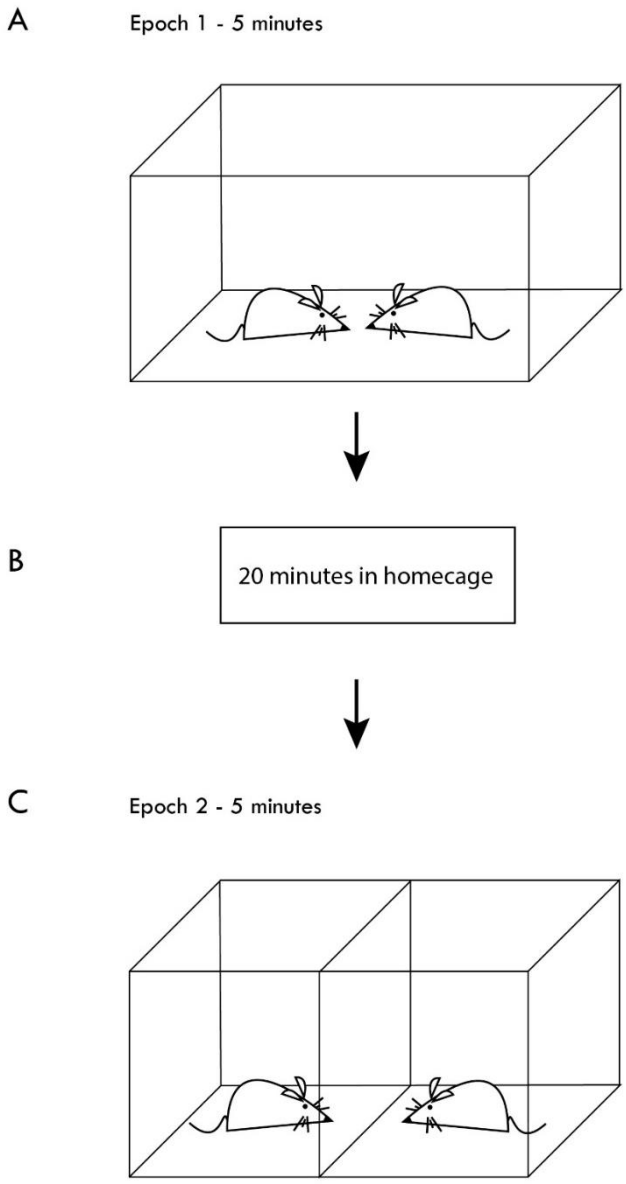

Figure 6. Experimental setup

A. Epoch 1 (INT) – Mice were allowed to directly interact with each other for 5 minutes. **B.** Undisturbed home cage period – allows for *Arc* to express and disperse into cytoplasm. **C.** Epoch 2 (OBS) – Mice observe each other through a non-perforated separator for 5 minutes.

2.2 Tissue Preparation

2.2.1 Maximum Electroconvulsive Shock

(The maximum electroconvulsive shock (MECS) step was carried out by Burke Lab at the University of Florida)

From Burke lab's protocol - McKnight Brain Institute, University of Florida, Gainesville, FL, USA:

The MECS was utilized to maximize *Arc* gene transcription in the positive control mouse. The animal was under isoflurane anaesthesia and placed on a heating pad during the procedure.

The animal was kept under anaesthesia with 1.5% isoflurane at 0.8 L/min flow rate. The MECS was carried out with the rodent electroconvulsive shock machine (Type 221; Hugo Sachs Elektronic, Gruenstrass, D79232 March Hugstette, Germany).

The shocks were delivered through saline soaked gauze pads on animal's ears with a 70 mA current for 0.3 seconds.

Five minutes after the shock delivery, the animal was placed in 5% isoflurane. After deep anaesthesia, the animal was sacrificed by cervical dislocation and the brain was removed.

cDNA for making RNA probes (described in Methods 2.3.3.1) was originally obtained from the reverse transcribed *Arc* RNA taken from the hippocampal region of the MECS animal. Also, tissues from the MECS animal were scanned with a fluorescence microscope (BZ-X 800, Keyence) to inspect if the in situ hybridization process worked (Supplementary Figure 1).

2.2.2 Snap Freezing

The brains of the animals were snap frozen immediately after the behavioural experiments. To do this, we used dry ice-chilled isopentane. Specifically, a 500 ml beaker was placed in the middle of an ice-filled styrofoam box. A smaller 100 ml plastic beaker was attached to the rim of the larger beaker via a binder clip. The larger beaker was filled with 100% ethanol, and dry ice was added to the 100% ethanol. After the bubbling reaction of ethanol ceased, the 100 ml beaker was filled with isopentane, bringing it down to ca. -78°C.

Immediately after the second behavioural epoch (OBS), the animals were placed in an isoflurane filled chamber, while cage control animals were placed in an isoflurane chamber directly from their home cages. Animals were sacrificed by cervical dislocation within 15 seconds of being overdosed with isoflurane. The brains of each pair of animals were rapidly extracted simultaneously, with the time difference being less than 30 seconds; the extraction time for the brains was five minutes on average.

The brains were immediately dropped in the chilled isopentane for snap freezing. They were removed after two minutes and placed carefully in labelled zip lock bags, which were then placed in brain cups. The brains were kept in a -80°C freezer until they were shipped to the Burke Lab in McKnight Brain Institute, University of Florida.

The brains were shipped to the collaborating lab with a specialized liquid nitrogen-cooled dry pod, which kept the tissues at ca. -180°C (Cryoport, USA).

The tissues from the positive control animal (MECS mouse) were collected in a similar manner as those at the Kavli Institute and cryopreserved by Burke Lab.

2.2.3 Sectioning

(Sectioning and mounting were carried out by Burke Lab)

A cryostat (Leica CM 1860) was used for cutting the brains into 20 µm thick coronal sections in two series, with tissue collection starting at the rostral end of the brain and proceeding caudally.

Brains were separated in two blocks, with each block containing three experimental brains, one of the control brains and one hemisphere from the MECS animal.

Sections were mounted on super frost plus microscope slides (Fisher Scientific 12-550-15) according to their blocks and placed in slide boxes with two dricap dehumidifiers (Type14, Ted Pella, Inc.). Series one and two were placed in different boxes, which themselves were placed in a -80°C freezer until the hybridization process.

2.3 In Situ Hybridization and Staining Procedures

All steps of the in situ hybridization process were carried out in Burke Lab. The protocols, reagents and equipment were provided by Burke Lab, McKnight Brain Institute, University of Florida, Gainesville, FL, USA.

2.3.1 DAPI Staining

Every 10^{th} slide from series one was removed from the slide box for DAPI staining.

The slides were moved from the -80°C freezer to a -20°C freezer where they were kept overnight. Slides were gradually thawed to room temperature over approximately 5 hours prior to staining.

Slides were then placed on a dipping rack and put in 4% paraformaldehyde solution for 10 minutes to fix the sections. The dipping rack was removed and rinsed in phosphate buffered saline (PBS) for two minutes. The slides were then moved to a fresh PBS solution for a second rinse.

For staining, slides were moved from the PBS solution to an opaque tray filled with PBS. For each slide, 110 µl DAPI solution was applied and the slides were coverslipped immediately. After a 30-minute incubation period in the opaque tray, the coverslips were removed and the slides were placed in PBS on a dipping rack for five minutes. Then, the slides were put in a second PBS container for two minutes. After PBS rinsing, Vectashield mounting medium was

applied to each of the slides. The edges of each coverslip were sealed with clear nail polish after approximately 24 hours. The slides were placed in an opaque slide box and kept in a 4°C refrigerator.

2.3.2 Section Selection and Delineation

Delineation and selection of the sections were completed in two steps.

First, a fluorescence microscope (BZ-X 800, Keyence) was used to collect 20x images of the DAPI stained slides. The sections were delineated for M2, dACC and vACC according to the Paxinos and Franklin Mouse Brain Atlas (2012).

These sections were used to determine the anterior and posterior borders for the brain regions in question.

Sections for in situ hybridization were selected from series one and two between the previously determined borders. Selected sections were delineated after the in situ process and before the final image collection for cell counting (Supplementary Figure 2).

Bregma levels from ca. +1.0 to +0.50 were selected for data collection in line with previous literature on the ACC in mice (Allsop, Wichmann et al. 2018).

2.3.3 In situ Hybridization

To avoid genetic or RNAse contamination of the samples, all equipment and surfaces were wiped with RNAse Away RNase inhibitor and rinsed three times with UV treated nuclease free water for all in situ hybridization steps. Ultra-pure nuclease free water was used for every solution, including rinses in water.

The RNA riboprobes were prepared beforehand, and the integrity was verified with 1% agarose gel prior to the in situ staining procedure. For the *Arc* catFISH procedure, the selected sections were processed over three days in pre-hybridization, hybridization, and post-hybridization steps. Pre-hybridization and hybridization steps were completed on day one. Days two and three finalized the catFISH process with post-hybridization steps.

2.3.3.1 RNA Probe

A riboprobe kit including a T7 RNA polymerase was used for the probe synthesis. Dioxigenin (DIG) RNA labelling mix was added to the reaction tubes (attached to every uracil nucleotide) for detection during the immunocytochemistry process. RNA was synthesized with the enzyme from the kit and cDNA was obtained from the MECS animal. The DNA template was removed by the DNAse from the same kit, and the riboprobe was purified subsequently with quick spin columns.

2.3.3.2 Pre-hybridization

Selected slides were fixed in 4% PFA for 10 minutes at room temperature and then rinsed in saline sodium citrate solution (SSC).

The slides were put in acetic anhydride solution then rinsed with water. Acetyl groups mask polar groups in the tissue to avoid weak bonds between the RNA probe and background molecules. After rinsing with water, the slides were placed in acetone-methanol solution at -20°C for five minutes to allow the probe to penetrate into the tissue. Slides were then rinsed in SSC to get rid of the residual acetone-methanol.

A pre-hybridization process is also needed to prevent or minimize nonspecific binding of RNA probes to irrelevant molecules in the tissue. The pre-hybridization buffer includes bovine serum albumin (BSA) which is utilized as a blocking agent for non-specific binding sites in the tissue. Essentially, the pre-hybridization buffer contains everything that hybridization buffer does with the exception of the riboprobe. The slides were treated with 50% pre-hybridization buffer and 50% de-ionized, nuclease free formamide solution and coverslipped. They were placed in an opaque tray and left to incubate at room temperature for 30 minutes.

2.3.3.3 Hybridization

The riboprobe was then hybridized with the mRNA in the tissue. To make the hybridization buffer, the riboprobe was added to 50% hybridization buffer and 50% de-ionized, nuclease free formamide and the solution was vortexed. The slides were rinsed in SSC and treated with hybridization buffer with the RNA probe, coverslipped, and placed in a 56°C oven for 18 hours in an opaque, air tight tray.

2.3.3.4 Post-hybridization

Reducing the Background Noise

Perfectly bound probe-RNA pairs (signal) are more stable than non-specific bonds between the probe and irrelevant sequences (noise). The post-hybridization steps aim to break the weak, irrelevant background bonds of the probe with a series of low stringency (high salt concentration) and high stringency (low salt concentration) SSC washes.

Specifically, slides were washed in a series of low stringency, 2X SSC washes to break non-specific bonds. They were then treated with RNAse to get rid of residual probe and reduce noise, then rinsed with SSC. Stronger non-specific bonds were broken with a series of high stringency 0.5X SSC washes.

Slides were washed with a 2% H_2O_2 and SSC solution to quench residual endogenous peroxidase activity, which prevents them from binding to anti-DIG molecules. Final washes were done with SSC and tris buffered saline (TBS).

Signal Amplification

The slides were treated with tyramide signal amplification (TSA) blocking buffer and 5% normal sheep serum, and incubated at room temperature for 30 minutes in an opaque tray. After incubation, the coverslips were removed and the slides were treated with HRP conjugated anti-DIG antibody diluted in TSA blocking buffer. The HRP-tagged anti-DIG antibody binds to the DIG attached to the uracil nucleotides in the RNA probe, thus amplifying the signal. The slides were left to incubate at 4°C for 18 hours.

Fluorescence Staining

The 3rd day of post-hybridization steps involved additional series of washes and staining. Slides were washed in series of TBS and 0.5% Tween-20 solution (TBS-T). Tween-20 is a mild detergent that breaks down membranes, which facilitates the penetration of the fluorophore Cy3 into the tissue to bind the HPR-tagged antibodies.

After the TSB-T washes, the slides were treated with Cy3 solution in an opaque tray at room temperature for 30 minutes, allowing Cy3 to bind to the HRP molecules.

The slides were then washed in TBS-T solution (2 x 10 minutes), followed by a 1 x 5 minute final wash in TBS. After the washes, sections were counterstained with DAPI (see DAPI procedure, Methods 2.3.1). After a 30 minute incubation period, the slides were coverslipped with Prolong Gold mounting medium and placed in a 4°C refrigerator for 24 hours before imaging.

2.4 Imaging and Processing

2.4.1 Imaging the Samples

A fluorescence microscope (BZ-X 800 All-in-One Fluorescence Microscope, Keyence) was used for image collection.

Z-stacks were taken with a 40x lens on 1.5 zoom, and in 0.7 µm increments. Two channels were set for Cy3 (566nm) and DAPI (457nm). The areas of interest were divided in superficial and deep layers, and two stacks were taken for superficial and deep layers in M2. A Single stack was taken per superficial and deep layers for dACC and vACC (Figure 7).

The 20x overview images were taken with a fluorescence microscope (Axio Imager, Carl Zeiss, Germany).

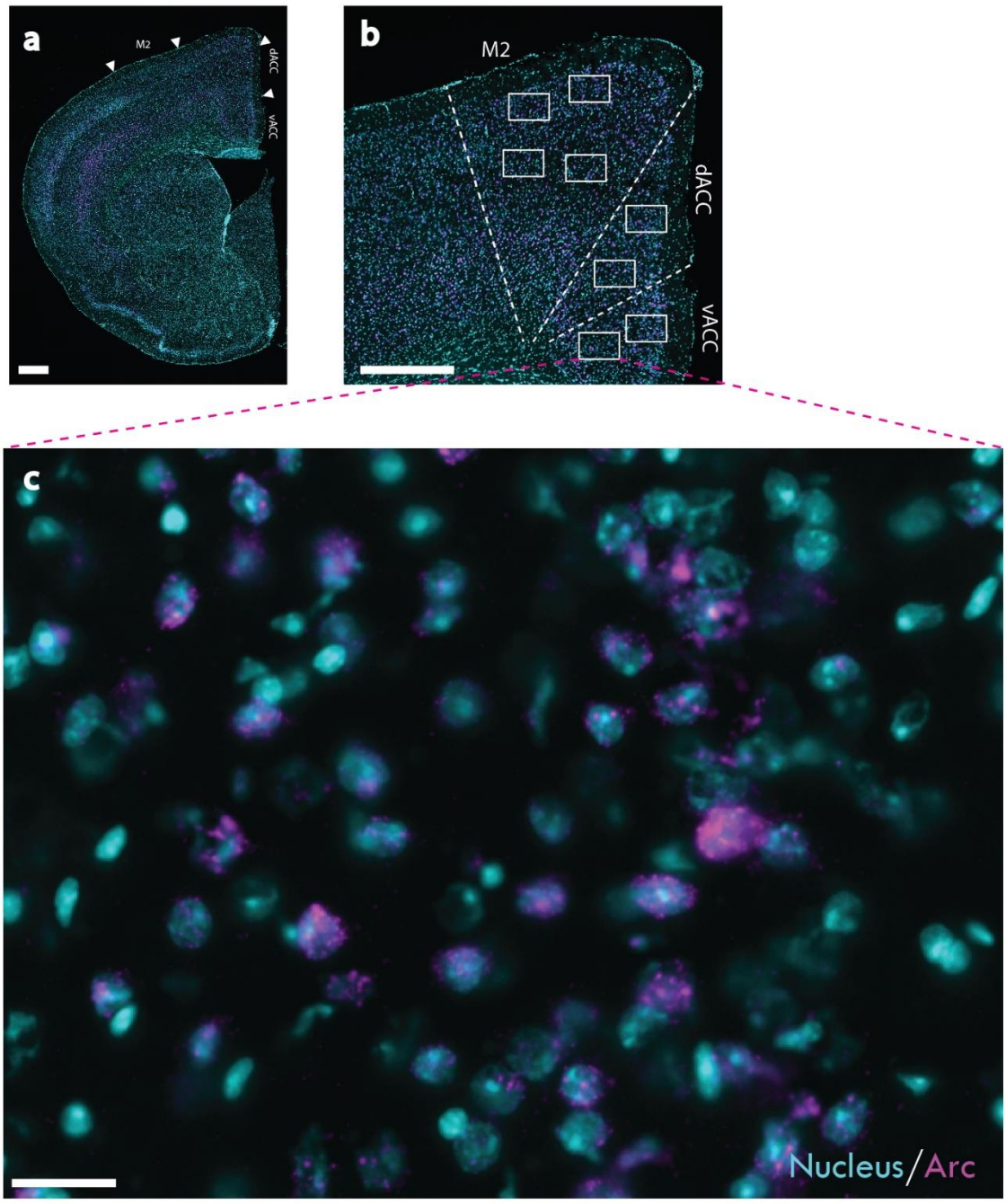

Figure 7. Generating Z-stacks

A. Overview scan of an example section used for data analysis. Scale bar = 500 µm. **B.** Close up of the delineated brain areas; white rectangles mark approximate positions for z-stacks. Scale bar = 500 µm. **C.** One frame taken from a z-stack. *Arc* mRNA is tagged with Cy3 (magenta) and nuclei are counterstained with DAPI (cyan). Scale bar = 25 µm.

2.4.2 Cell Counting for Analysis

The cell counting and localization of *Arc* mRNA were executed manually using ImageJ software (version 1.52a) with the cell counter plugin. Prior to counting, the folders and files were randomized to minimize bias.

To ensure that nuclei were not cut off by stack boundaries, only cells that were visible in the median 20% portion of the stacks were included for counting. For example if a stack consisted of 25 planes, only 5 planes in the middle of the stack would be counted. This procedure also prevented oversampling of cells that might be visible on adjacent stacks. Glia were excluded as these cells do not have *Arc* expression. Glia are typically smaller than principle cell nuclei and they are more saturated. They also look more uniform and smoother compared to highly textured nuclei (Figure 8A).

The nuclei were counted with the *Arc* channel turned off to remain unbiased. Evaluation of *Arc* positive cells was determined after the nuclei count was finalized.

The *Arc* mRNA signal appears as intensely coloured dots in the nucleus (magenta; Figure 8B). Cells in which *Arc* mRNA signal was confined to the nucleus were labelled as “foci +”; there could be one or two foci in the nucleus depending on whether both copies of the *Arc* gene were transcribed or not. The *Arc* signal should also have been visible on at least four adjacent planes to qualify as “foci +” (Figure 8B).

The cells that had *Arc* mRNA only in the cytoplasm were labelled as “cyto +.” In these cases, *Arc* signal should surround at least one third of the nucleus and follow the contour of the nucleus of the cell (Figure 8C).

Cells in which *Arc* signal appearance satisfied both cyto and foci-positive criteria were labelled as “both” (Figure 8D).

Cells which had no *Arc* expression were labelled as “negative.”

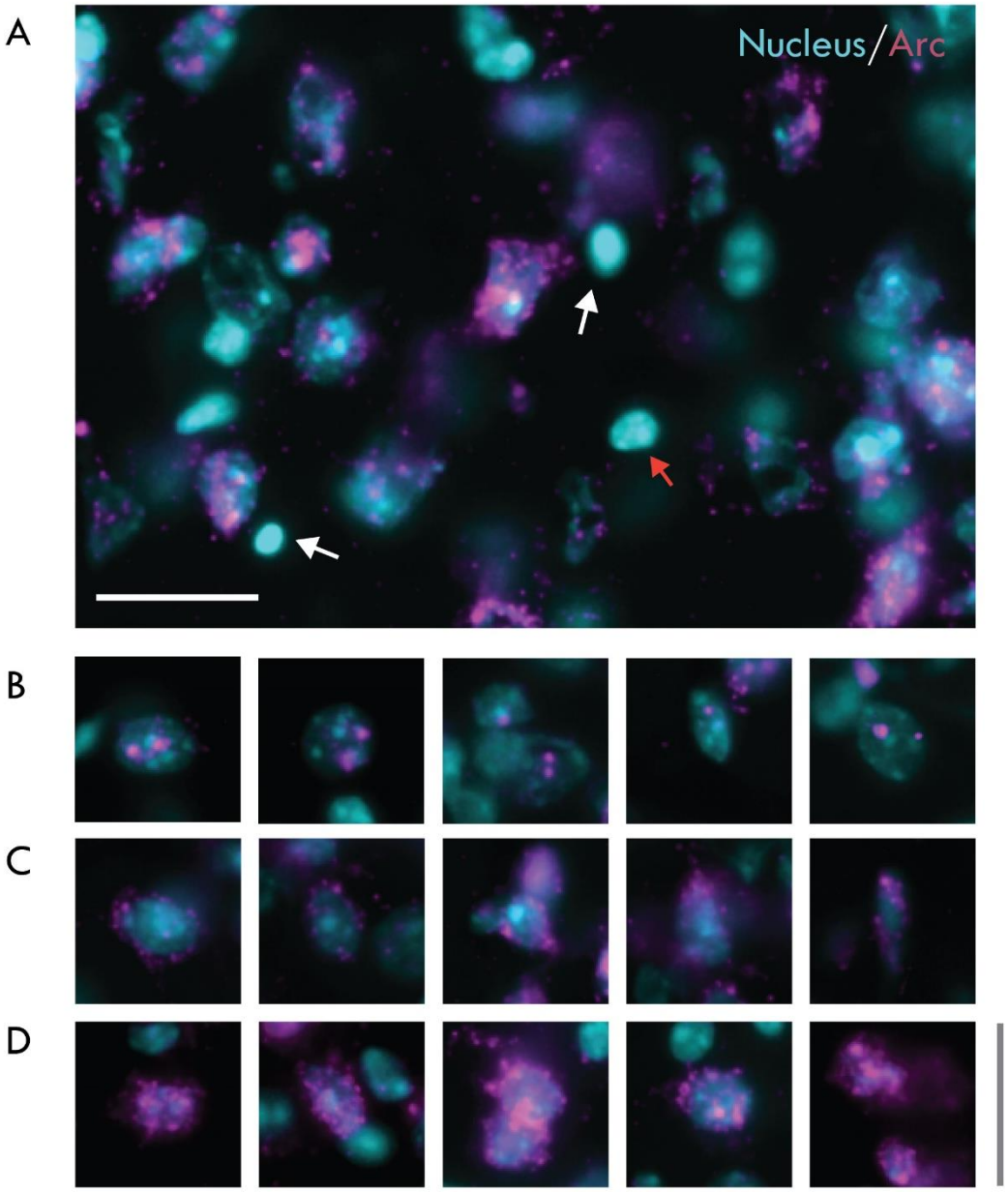

Figure 8. Cell counting criteria

A. A small portion of one plane from a z-stack; nuclei are coloured cyan and *Arc* signal is magenta in all panels. White arrows indicate glia, which appear dense, saturated and typically smaller and less textured than principle cell nuclei. Some small and compact nuclei may appear similar to glia, however, they are more textured than glia (example of a compact nucleus is marked with a red arrow). Scale bar = 25 µm. **B.** Examples of "foci +" cells. *Arc* signal appears as intense colour deposits (magenta). **C.** Examples of "cyto +" cells, where *Arc* signal only appears in the cytoplasm, and follows the contour of the cell nucleus. **D.** Examples of cells where *Arc* signal satisfies all criteria of "foci +" and "cyto +" cells, and qualify as "both". Grey scale bar at the bottom right = 25µm, same for B, C, D

2.5 Methods Workflow

Figure 9 shows the methods workflow leading up to the data analysis step.

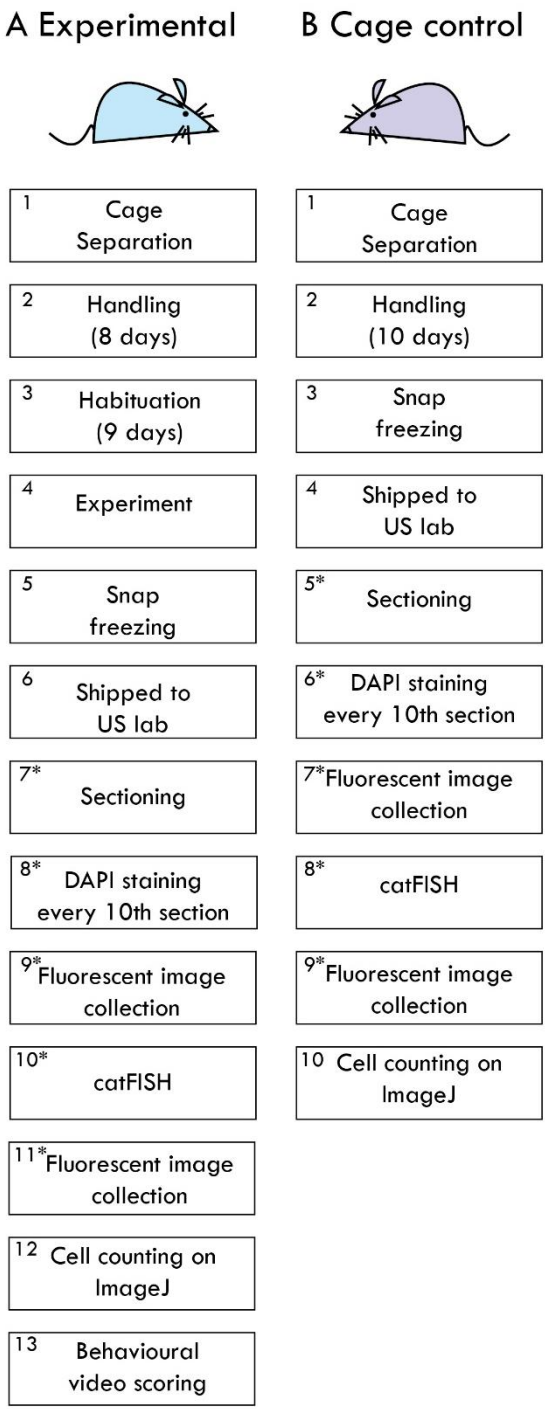

Figure 9. Methods workflow

A. Methods workflow for experimental animals. **B.** Methods workflow for cage control animals. Asterisks (*) mark steps that were carried out in the Burke Lab at the University of Florida.

2.6 Data Analysis and Statistics

2.6.1 Behavioural Scoring from Experiment Videos

The interactions between experimental animals were quantified by scoring videos of experiment frame by frame. The videos (each 5 minutes, ca. 9000 frames) were opened with Fiji App (version 1.51h) and frames that fit specific interaction criteria were marked for each epoch.

For epoch 1 (INT), the frames in which the animals were in direct contact with each other were marked as “Interaction”. In epoch 2 (OBS) the observation time was different for each animal. Hence, the epoch 2 (OBS) video was scored separately for each experimental mouse. The frames were marked as “Observation” when the animal was directly adjacent to the separator and its head was facing toward the conspecific (Figure 10B). Intervals when the animals were neither physically touching nor facing toward the other animal were marked “Irrelevant”.

2.6.2 Statistics

2.6.2.1 Main Analysis

A factorial ANOVA is typically used in classic *Arc* catFISH literature (Guzowski, McNaughton et al. 1999, Burke, Chawla et al. 2005). However, due to time and resource constraints in the project, the sample size (two animals per condition) of the study did not satisfy ANOVA assumptions. Thus, a chi-square test was used for comparison of the occurrence of “foci +”, “cyto +” or “both” categories for *Arc* expression in the experimental (EXP) and cage control animals (CC). Three pairwise chi-square tests were used for comparison of brain regions from experimental animals (M2-dACC, M2-vACC, dACC-vACC). Since we did not observe differences between *Arc* expression patterns in deep and superficial layers, cell counts from superficial and deep layer z-stacks were compiled for the analysis.

To determine the statistical significance of differences in cell counts across behavioural categories a chi-square test was applied to the total cell counts. The differences in cell counts between conditions can lead to over or underestimation of differences because chi-square test uses frequencies instead of proportions so we equalized the number of cells for conditions with proportions remaining the same. In that regard, proportions of “foci +”, “cyto +”, “both”, and “negative” were calculated for total cage control cell count. These proportions were then applied to the total experimental cell count and the resulting frequencies were used in the analysis as counts from cage control animals.

A similar approach was taken for pairwise chi-square tests for comparing *Arc* signal across brain areas in experimental animals. Three pairwise tests (M2-dACC, M2-vACC, dACC-vACC) were applied to compare differences. For each test an area was chosen as an anchor to equalize cell counts.

The chi-square test is sensitive to small differences and typically does not indicate which category drives the significance. Thus, a pseudo factorial ANOVA test was further applied to the data in order to verify and assist our interpretation of the chi-square results. Cell counts

for each brain region were compiled per hemisphere (nine hemispheres per condition). The percentages from resulting sums were used for ANOVA. The data points were also utilized for data visualization.

2.6.2.2 Similarity Scores

Similarity scores are generated to reduce four values of cell evaluation (foci +, cyto +, both, negative) to a single numerical value to compare activity patterns of different brain regions.

The similarity scores per hemispheres were calculated according to the previous definitions (Vazdarjanova and Guzowski 2004, Burke, Chawla et al. 2005, Hernandez, Reasor et al. 2018).

Similarity score (SS) is calculated as:

$$SS = \frac{p(B) - p(E1E2)}{\frac{p(E1) + p(E2)}{2} - p(E1E2)}$$

p(E1) = proportion of “cyto positive” + proportion of “both”

p(E2) = proportion of “foci positive” + proportion of “both”

p(B) = proportion of “both”

p(E1E2) = E1xE2

The similarity score can range in value from -1 to +1. Higher scores indicate the activation of similar neural ensembles across epochs, such that a score of 1 would indicate that the exact same neural ensemble was activated by epochs 1 and 2. Lower similarity scores indicate activation of more independent neural ensembles across behavioural epochs. Specifically, a score of 0 indicates that statistically independent cell populations were activated in each epoch, and a score of -1 indicates that no cells were activated in either the first or second behavioural epochs.

Chapter 3

Results

3.1 Interaction and Observation

During epoch 1 (INT), animals were free to interact with each other and did so for 61% of the 5-minute session (Figure 10A). Interaction behaviours included sniffing (anogenital and other) and social grooming. One of the animals (EXP2) was more active and investigative than the other one (EXP1), with EXP2 mostly initiating social grooming and sniffing behaviour. The animals did not show any signs of stress during the interaction epoch, and when they were not in contact with each other their behaviour included normal self-grooming and exploration of the cage.

Epoch 2 (OBS) scores of experimental animals were also comparable (Figure 10 C.1 and C.2). Similar to epoch 1, neither animal showed any signs of stress during epoch 2 (OBS). Their behaviour included normal self-grooming, some rearing and cage exploration.

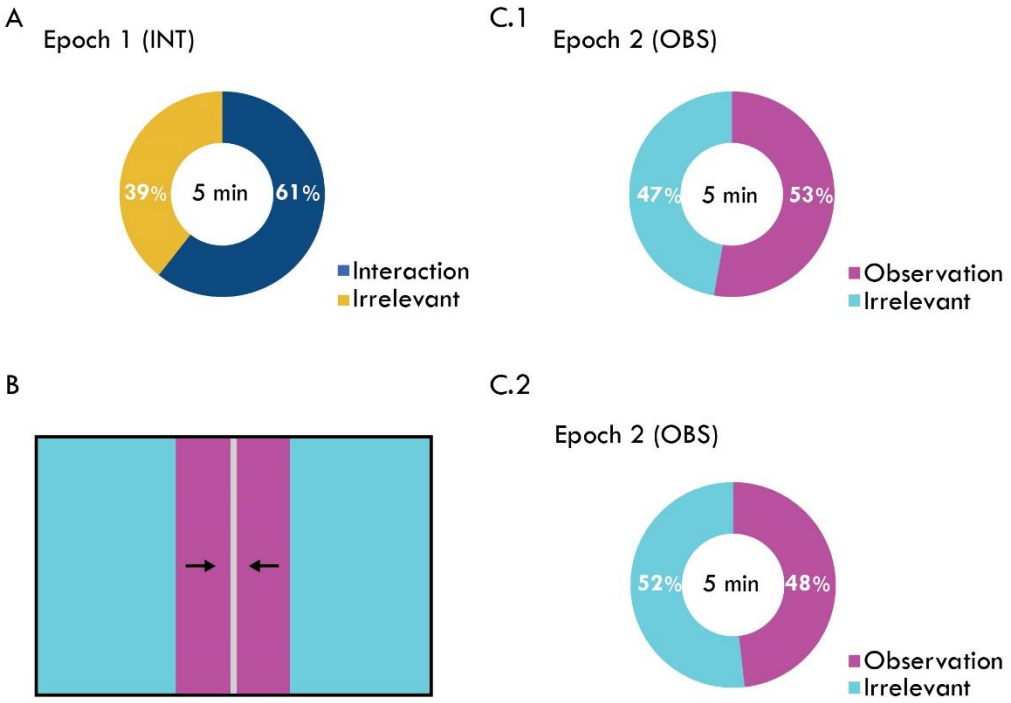

Figure 10. Behavioural scoring of experiment videos

A. Epoch 1 scores. Frames in which the animals interacted were marked as "Interaction" (blue). **B.** Criteria for epoch 2 (OBS) scoring. When the animal was in the area nearest the cage divider (magenta zone) and it was positioned toward the other animal, the frames were marked as "Observation." Black lines represent the cage and the grey line in the middle represents the separator. **C.1.** Observation time for EXP1. **C.2.** Observation time for EXP2 (the more socially active animal).

3.2 Main Cell Count

24,089 cells were counted and evaluated across brain regions in total (Table 2).

	M2			dACC			vACC		
	Total	Mean	SD	Total	Mean	SD	Total	Mean	SD
Cage Control	5714	634.89	61.28	3048	338.67	32.71	3064	340.44	41.79
Experimental	5385	598.33	148.22	3034	337.11	26.78	3844	427.11	39.46

Table 2. Total cell count

Total cell counts for the brain regions in question. Mean and standard deviation were calculated per hemisphere.

Pearson's correlation test did not reveal significant correlation between the number of cells counted and the proportion of *Arc* positive cells for all behavioural conditions and brain regions ($p>0.01$ for all, $R=0.39, -0.19, 0.22$ for M2, dACC and vACC, respectively for control condition and $R=0.15, -0.22, -0.49$ for experimental condition).

Percentages were calculated from total cell counts per hemisphere and used as data points. Figure 11 shows the distribution of percentages of *Arc* expression categories (foci +, cyto +, both).

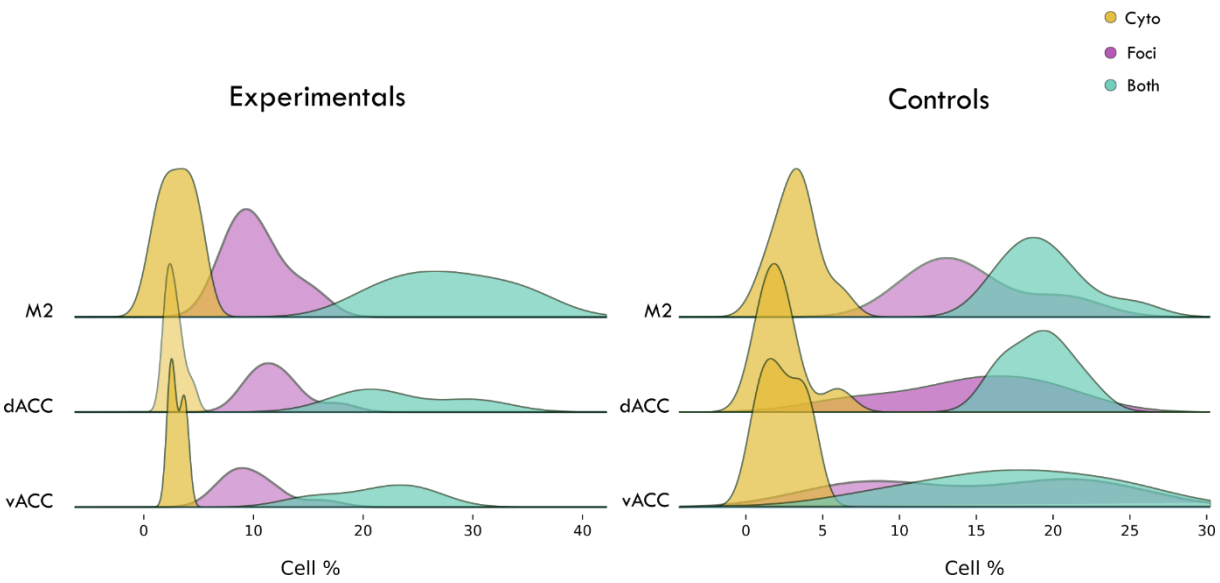

Figure 11. Density plot showing percentages of cells in different Arc *expression categories*

Distribution density of *Arc* positive cells (foci +, cyto +, both). The category "negative" was taken into account for analyses but not shown on the graph.

3.3 *Arc* Signal Distribution

3.3.1 Comparison of Experimental Animals (EXP) to Cage Controls (CC)

To determine if the overall frequency of *Arc* expression was higher or lower in experimental *vs.* control animals, the expression categories (foci +, cyto +, both, negative) were pooled across regions (M2, dACC, vACC) for CC and EXP.

The chi-square test showed that the *Arc* signal distribution (foci +, cyto +, both, negative) in cage control (CC) and experimental (EXP) animals were significantly different (X^2 (3, N=24526) = 396.07, $p < 1.0e^{-20}$ (Figure 12)).

Cell count proportions of “foci +” and “both” had the largest difference. “Foci +” proportions were 0.15 and 0.11 for control and experimental groups, while "both” were 0.19 and 0.25 for CC and EXP, respectively. “Cyto +” proportions were the same for CC and EXP at 0.03.

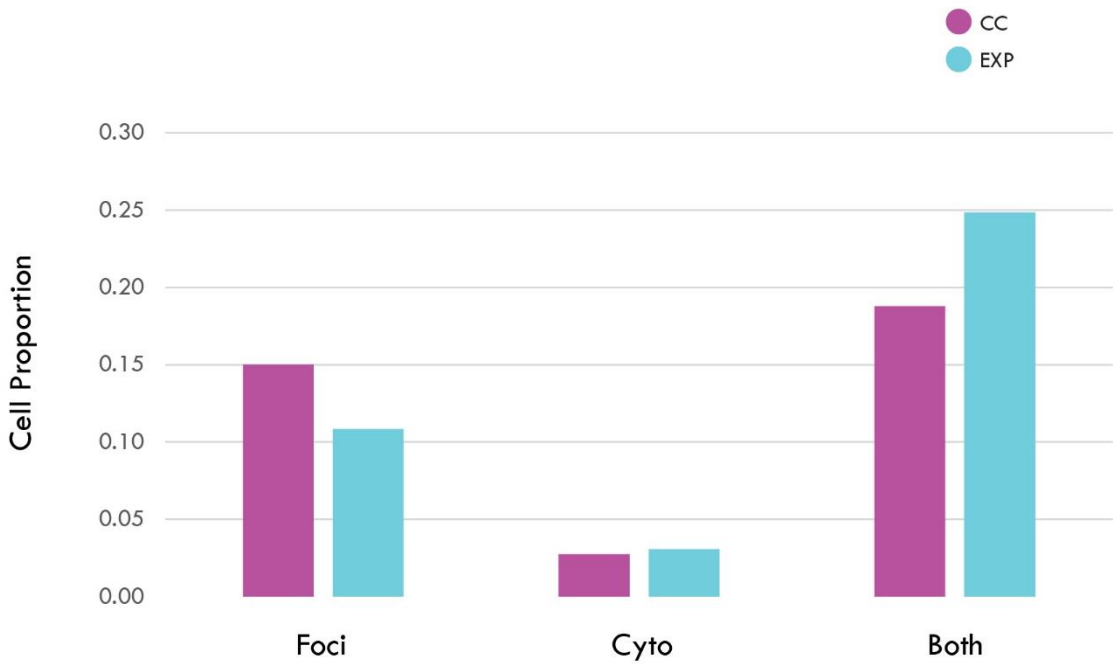

Figure 12. Proportions of cells in experimental animals vs cage controls – Chi-square *results*

Proportions of “foci +”, “cyto +”, and “both” for experimental and cage control animals. Largest differences were “foci +” and “both”. The “negative” category was also included in the chi-square calculations (with proportions of 0.61 and 0.64 for CC and EXP, respectively), but is not shown. Chi-square test indicated the overall difference was highly significant (see main text).

The region identities were disregarded in the chi-square analysis because the factorial ANOVA results suggested no significant differences between M2, dACC and vACC (Supplementary Table 1). On the other hand, ANOVA and Tukey HSD results revealed a significant interaction effect of condition (CC, EXP) and category (foci +, cyto +, both) ($F(2,144)=23.4$, $p<0.05$) (Figure 13). According to the results:

a) EXP has higher "both" activation than CC.
b) CC has higher foci (+) activation than EXP.

These results support that the chi-square significance was driven by both "foci +" and "both" differences, which is evident in the comparisons as shown in Figure 13:

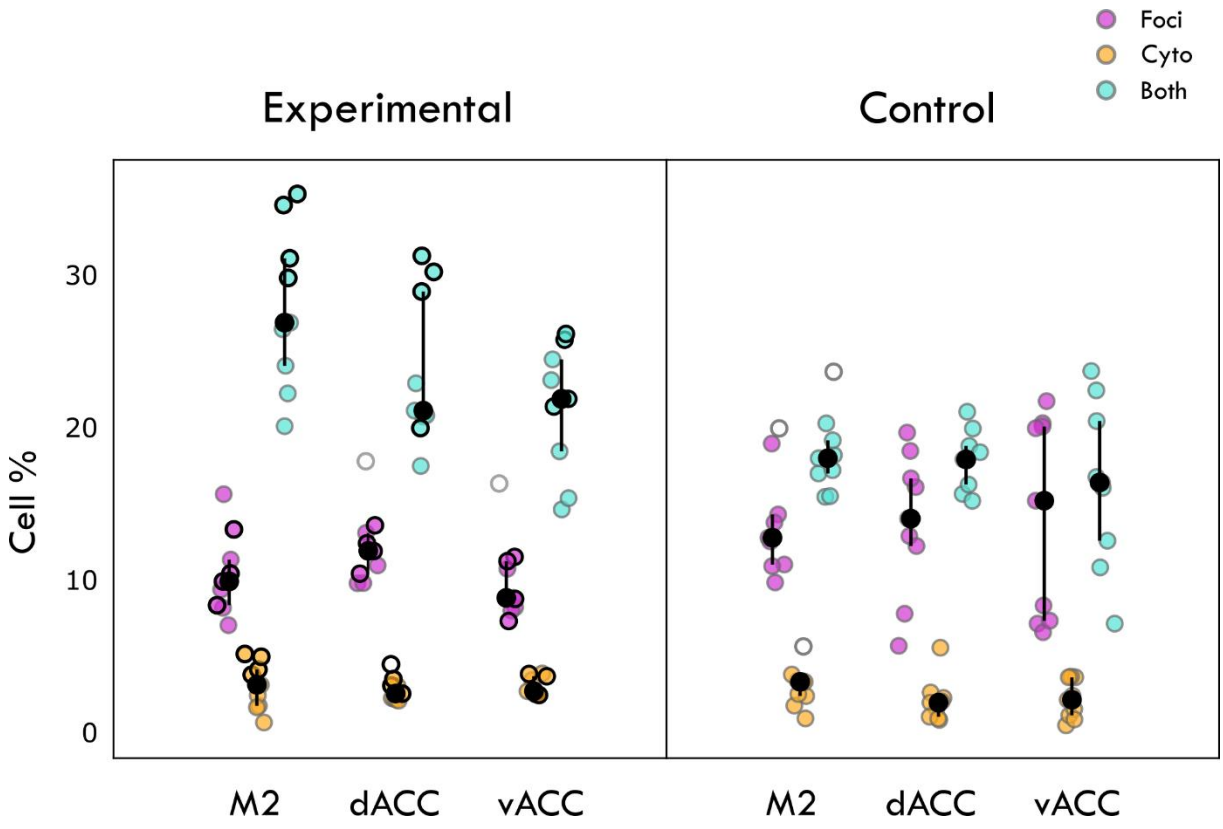

Figure 13. Percentages of cells in different categories for Arc expression in experimental animals vs cage control animals.

Cell percentages for EXP and CC. Black circles mark the median and whiskers indicate the interquartile range for each comparison; ***individual circles correspond to data from each hemisphere***; outliers are shown as open circles. The data points outlined in black in the EXP group came from EXP2, which was more interested in direct social contact (Results 1).

Cell counts for M2, dACC, and vACC were pooled *per hemisphere*, and cell percentages were calculated using the resulting cell counts.

The results suggest that even though social interaction had an effect on activation in M2 , dACC and vACC, the activation of these areas had no preference for either epoch 1 (INT) or epoch 2 (OBS).

Higher "foci +" activation in CC indicates possibility of uncontrolled activation in CC animals just before sacrifice (see Discussion for more detail).

3.3.2 *Arc* Distribution Comparisons across Brain Regions in Experimental Animals

Having shown that social interactions caused significant changes in the pattern of *Arc* expression relative to control animals, we next wished to determine if the effects were larger for a particular category of *Arc* expression in any of the three brain regions considered. Since the number of data points was not sufficiently high to meet the assumptions of an ANOVA, we instead conducted three pairwise chi-square tests across brain regions (M2-dACC, M2-vACC, dACC-vACC). Cell counts were pooled from all z-stacks for each brain region for the tests. The chi-square tests for each regional comparison were significant, with the "both" category showing the largest difference between groups (Figure 14).

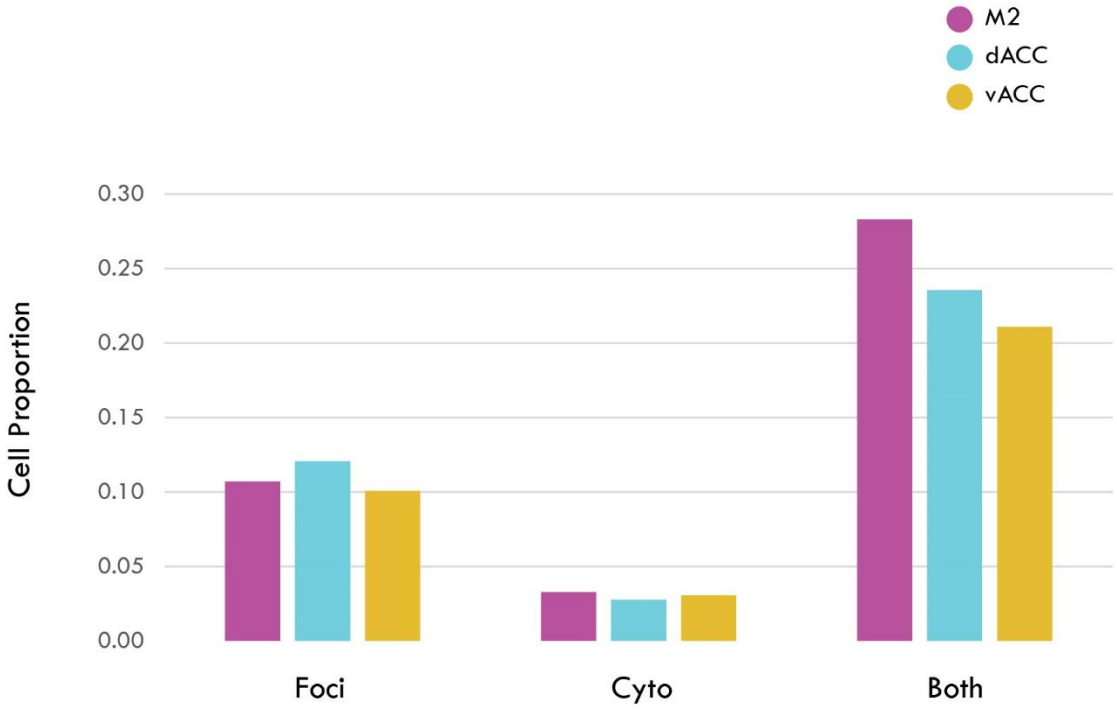

Figure 14. Comparisons across brain regions (for experimental animals)

Cell proportions of "foci +", "cyto +", and "both" for M2, dACC, and vACC from experimental animals. All three chi-square tests were significant, indicating that M2, dACC and vACC had different *Arc* signal distribution patters for the behavioural epochs. The category "negative" was included in the calculations but not shown on the graph. The results for each chi-square tests were:

M2-dACC X^2 (3, N=5,385) = 78.40, p = $1.11e^{-16}$

M2-vACC X^2 (3, N=5,385) = 116.79, p < $1.0e^{-20}$

dACC-vACC X^2 (3, N=3,844) = 29.54, p = $1.72e^{-06}$

Unlike the chi-square results, factorial ANOVA did not suggest any significant differences for brain regions (Supplementary Table 1) as chi-square is mathematically more sensitive because the difference between the values is squared in the formula. However as can be seen in Figure 13 the data points also show a trend in the same direction.

The fact that the size of the effect was largest for the "both" category indicates that although M2, dACC and vACC were activated for both epochs (INT and OBS) in similar ways, this activation happens to different degrees in each area suggesting region differences.

3.3.3 Similarity Scores

The pairwise chi-square tests for experimental animals were calculated with the total cell count of each category (foci +, cyto +, both, negative) pooled across z-stacks. The fact that "both" was higher than other *Arc* signal categories (foci +, cyto +) indicates similarity of activated neural ensembles across epochs. We next wished to determine how and to what degree this similarity was reflected for each hemisphere in the experimental animals.

As mentioned previously, CC animals had higher "foci +" levels than EXP animals. This could be attributed to uncontrolled stimuli prior to sacrifice. We also wanted to see how uncontrolled stimulus shifted the neural activity from baseline levels if that was the case.

This would also allow us to compare the similarity levels of unrelated shift from baseline and activation pattern of social interaction episodes.

To do this, similarity scores (SS) were calculated per z-stack and averaged for each hemisphere.

For all brain areas, the mean similarity scores were higher in the EXP than CC conditions. Specifically, for M2 the mean SS was 0.70 ± 0.07 (standard deviation) for EXP *vs.* 0.57 ± 0.07 for CC groups; for dACC it was 0.65 ± 0.05 for EXP *vs.* 0.58 ± 0.10 for CC; and for vACC 0.67 ± 0.08 for EXP *vs.* 0.55 ± 0.18 for CC (Figure 15).

The fact that similarity scores were higher for each comparison indicates that activation pattern caused by a suspected random stimulus is less similar to baseline levels than behavioural epochs are to each other. It was not appropriate to perform further statistical analysis on the data because CC animals were not behaviourally matched controls.

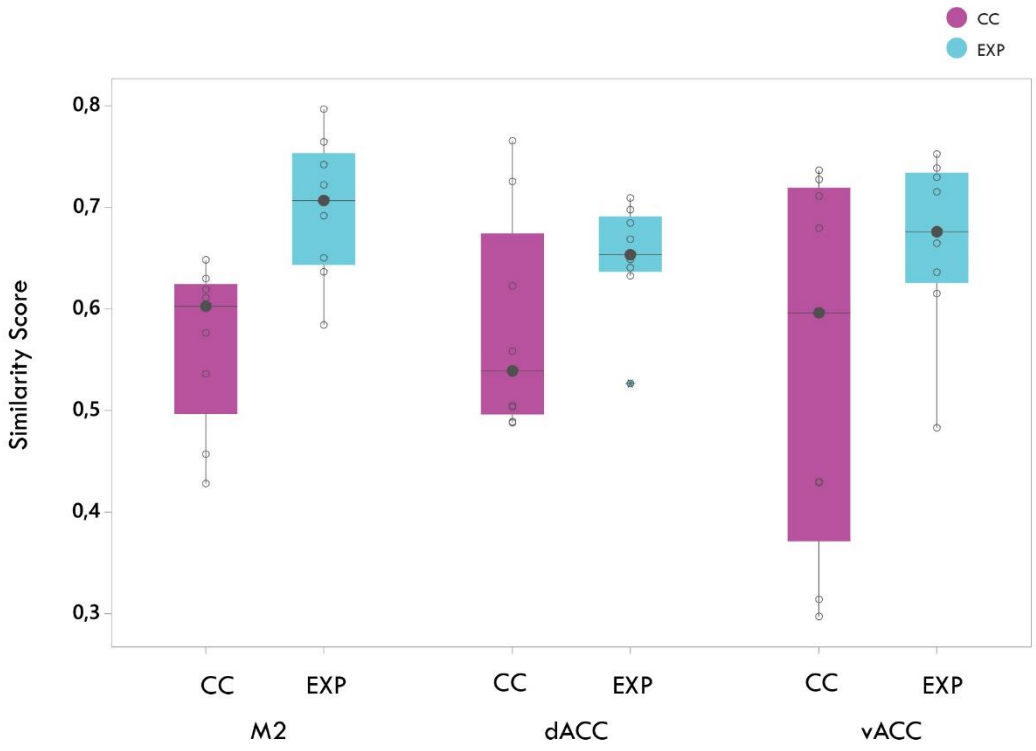

Figure 15 Similarity scores for each brain region in experimental and cage control groups.

Box and whisker plots of similarity scores for EXP and CC group. The horizontal line in each box marks the median, boxes indicate interquartile range and whiskers extend to minimum and maximum data points. The outliers are marked with asterisks. The SS was higher in the EXP than CC group for each comparison.

Higher similarity scores indicate that similar neural ensembles were activated by both epochs. Lower similarity scores indicate that more distinct neural ensembles were activated by epochs 1 and 2.

Chapter 4
Discussion

4.1 Summary of the Results

As described in previous literature, M2 and ACC are association areas which are anatomically and functionally implicated in social cognition in rats and mice (Barthas and Kwan 2017, Allsop, Wichmann et al. 2018, Ebbesen, Insanally et al. 2018, Carrillo, Han et al. 2019).

The aim of this study was to investigate whether ACC or M2 had preferential representation of a conspecific during interactions allowing tactile contact and those that do not, and *Arc* catFISH was chosen as the method to capture the representation of two behavioural episodes in the brain of the same animal.

Frame-by-frame labelling of the behaviour videos showed that animals interacted with each other 61% of the INT episode, and experimental animals observed the conspecific for approximately 50% of the time in the OBS episode.

A chi-square test comparing experimental animals to cage control animals revealed that the proportions of *Arc* signal (foci +, cyto +, both) were significantly different in each condition. Furthermore, a factorial ANOVA test supported these results with a significant interaction effect of condition (experimental vs. cage control) and *Arc* signal category (foci +, cyto +, both). Animals in the experimental condition had more “both” labelled cells than control animals. In contrast cage control animals had more “foci +” labelled cells. The proportion of *Arc* negative cells and “cyto” labelled cells were similar in both conditions.

A chi-square analysis also suggested a difference in the activation pattern in areas investigated (M2, dACC, vACC) in the experimental animals. M2 had the greatest amount of “both” labelled cells, followed by dACC and vACC.

Similarity scores indicated that the activation patterns in both experimental and control animals were highly similar (similarity scores >0.5 for *Arc*-positive cells in z-stacks) across the two epochs, but that experimental animals had higher scores than controls.

4.2 Methodological Considerations

Behavioural Considerations

As this study investigated naturalistic social cognition in mice, our intention was to enhance the novelty of social interactions, so animals previously housed together were not allowed to interact during the habituation phase of the experiment. This made predicting animal behaviour during the experiment challenging. Since experimental pairs were siblings, they were reared and housed together until being moved to separate cages prior to the habituation period. Because of their kinship and familiarity, we predicted that fighting would be minimal in line with previous literature (Kareem and Barnard 1982), but some pairs had continuous aggression in the form of fighting during the INT epoch in the experiment. These animals were excluded from the analyses because the scope of this study sought to cover prosocial interactions.

Other Sensory Information

Olfactory and auditory information is also essential for perception of an environment for rodents (Calhoun 1963). However, it was beyond the scope of this study to cover sensory information beyond touch and vision, so auditory and olfactory information were left constant in both behavioural episodes. The experimental cage was wiped with 70% ethanol and the bedding was changed during the 20-minute delay period to prevent any lingering scents from the previous epoch.

Snap Freezing

After the behavioural experiment the brains were snap frozen to maintain tissue integrity and to preserve them until cryosectioning. It was found, however, that this process can be damaging to the tissues in ways that could create problems during data collection and staining procedures. Specifically, the hemispheres of some brains physically separated at the corpus callosum due to the freezing process, leading to one hemisphere shifting in the anterior-posterior axis (Supplementary Figure 2). Thus, all hemispheres were delineated individually before imaging and counting.

Arc catFISH

Arc catFISH was chosen as the method for this study. The characteristics of the *Arc* gene transcription process allowed us to temporally distinguish two events separated by approximately 20 minutes in the same brain (see Introduction for more details), without any interference of surgical procedures, injections or head implants. The method also provides excellent control over the areas investigated in the study, as the mRNA detection is executed

post factum. This also allows us to explore other brain areas that might emerge as relevant to the same kind of stimulus and behavioural design at a later point, as long as the samples are kept dry and frozen at -80^{o}C until in situ hybridization process.

However, one caveat of the method for some experiments could be that the temporal resolution does not provide precise neural activation and behaviour coupling like electrophysiology or calcium recordings. Instead, catFISH provides a snapshot of the activity of a particular neural ensemble in response to ongoing stimuli rather than reporting exact instances where cells are firing. This requires keeping the relevant stimulus consistent during the behavioural episode and minimizing other stimuli that could be confounding. As mentioned in the methods, experimental animals were well habituated to the experimental set up and the experimenter. The cage was covered with opaque material and curtains were introduced to eliminate further visual cues about the environment.

mRNA detection using *in situ hybridization* is an arduous process that requires vigilance during the immunohistochemistry steps to prevent contamination from extraneous RNA or background staining due to non-specific bonds. Proper measures as described in methods were employed to minimize contamination and background signal.

Following FISH, the tissue was scanned, cells were counted and evaluated from scanned images. Also, the sections were mounted with a medium which helps preservation of fluorescent signal (ProlongGold), stored in an opaque box and kept in a refrigerator to minimize photobleaching.

The tissue thickness (20 µm) and the intense preparation required for catFISH made staining the same sections with Cresyl Violet extremely challenging, so instead all sections were delineated using DAPI-stained tissue.

4.3 Discussion of Results

4.3.1 Interaction and Social Status

The experimental animals freely interacted with each other during 61% of the 5-minute INT epoch, while during the observation period they spent approximately 50% of the 5-minute epoch observing the other animal. The behaviours during the INT epoch included previously described social interactions in mice such as sniffing and social grooming, and non-social behaviours included self-grooming, exploration and rearing (Kareem and Barnard 1982, Kingsbury, Huang et al. 2019).

Both animals had comparable locomotor activity and both exhibited similar social and individual behaviours. However, one animal (EXP2) initiated social interactions and especially social grooming more often than the other (EXP1). Social grooming (or allogrooming) and initiation of passive body contact has been associated with social hierarchy, particularly dominance in mice (Kareem and Barnard 1982). Extremely vigorous forms of social grooming

are defined as precursor of aggression (Kareem and Barnard 1982), so it can be said that EXP2 in this study had more dominant traits than its counterpart EXP1.

Interestingly, the more dominant animal had the highest scores in the category "both" for *Arc* expression in secondary motor cortex and dorsal anterior cingulate. This pattern was also repeated in the category "cyto", which corresponds temporally to the INT epoch, only in secondary motor cortex. It is tempting to interpret the data as relating to social status, which is an important feature that has been implicated in neural correlates of social interaction. For example, in a social interaction episode similar to the INT epoch of this study, the synchrony of activity in dorsomedial prefrontal cortex of socially interacting mice is higher if the two animals are more distant in the social hierarchy (Kingsbury, Huang et al. 2019).

Although it is not possible to infer synchrony from catFISH data, the differences in activation pattern might also reflect aspects of social status in M2 and dACC in mice.

4.3.2 Social Interaction Activates Secondary Motor and Anterior Cingulate Cortices

The factorial ANOVA test revealed that experimental animals had a greater number of cells in the "both" category than cage controls in all areas considered (M2, dACC, vACC). This activation pattern was also associated with both behavioural episodes (INT and OBS). In turn, the scores for "foci +" was lower and "cyto +" was the same.

As association areas, both M2 and ACC have extensive connections with cortical and subcortical areas, and both areas receive information from similar networks. These inputs include primary sensory cortices as well as "higher" association areas such as PPC and RSC, so M2 and ACC both receive primary and more highly processed sensory information (Zingg, Hintiryan et al. 2014, Barthas and Kwan 2017, Fillinger, Yalcin et al. 2017).

Briefly, M2 has reciprocal connections with visual areas and is associated with saccade like voluntary eye movements in mice. The area is involved in vibrissal motor behaviour, it has connections with somatosensory cortices and has motor neurons that respond to forelimb tactile stimulation (Ebbesen, Insanally et al. 2018). Unlike M1, M2 strongly receives information from PPC (Reep, Goodwin et al. 1990, Hovde, Gianatti et al. 2019, Olsen, Hovde et al. 2019) and is important for tactile interaction with other animals or their environment (Ebbesen, Insanally et al. 2018).

As for the ACC, it is strongly implicated in observational fear learning and social cognition particularly via visual input (Allsop, Wichmann et al. 2018, Carrillo, Han et al. 2019), and it too has been shown to play a modulatory function during tactile stimulus discrimination (Kunicki, R et al. 2019). We therefore thought it reasonable to find activation patterns that reflected a disassociation of the representations for visual and tactile social interactions. One possible expected pattern would have been higher "foci +" and "cyto +" counts in experimental animals reflecting the visual (OBS) and tactile (INT) interactions, respectively. One other alternative

would have been seeing higher “cyto +” and “both” levels, in case visual interactions also drove neural activation during INT epoch.

However, our results did not match these predictions, as “cyto +” levels were the lowest and they were at similar levels as control animals, whereas the number of cells labelled as “both” was higher in experimental animals. This indicates that both visual and tactile social experiences triggered strong neural activation in the areas investigated.

These results could lead to several interpretations regarding the pattern of neural activation. The simplest explanation would be that tactile information does not play a significant role in the representation of a conspecific in the particular brain regions investigated in this study (M2, dACC, vACC). However, this explanation seems unlikely in light of previous literature and the ethological relevance of tactile information to rodents.

It has been shown, for example, that initiation of whisking behaviour in social interactions is associated with decreased excitability of layer V descending-projection neurons in M2. This inhibition of layer V neurons leads to disinhibition of whisking behaviour in the brainstem target areas (Ebbesen, Insanally et al. 2018). However, as mentioned in results, there was no difference in “foci +”, “cyto +”, and “both” proportions between superficial and deep layers in any of the areas investigated, leading us to pool the data for analysis. Also, the “cyto +” proportion in M2 was very similar to both control animals and ACC areas in the experimental animals. Although, ACC in rats has been associated with eye and nose movements (Brecht, Krauss et al. 2004), the area has not been associated with decreased activation during tactile interaction to our best knowledge, in this particular study, the “cyto +” proportion associated with INT epoch is not likely to be explained by a whisking-related reduction in excitability.

In light of these observations, it is possible that M2, dACC and vACC respond to a conspecific with a general activation pattern rather than sensory-specific neural ensembles. These areas all receive highly processed sensory information from other association areas (Zingg, Hintiryan et al. 2014, Barthas and Kwan 2017, Fillinger, Yalcin et al. 2017, Hovde, Gianatti et al. 2019, Olsen, Hovde et al. 2019), so it is possible that processed tactile and visual information converge on the same cells in M2 and ACC.

A recent study with calcium imaging in mouse brain involving similar behavioural episodes (INT and OBS) revealed that dorsomedial prefrontal cortex (dmPFC) and prelimbic cortex (PL) show synchronous activity across interacting animals (Kingsbury, Huang et al. 2019). This synchronicity was observed during the INT epoch but was abolished when the animals were not allowed to touch each other, yet still had visual access to each other through a transparent separator (OBS) (Kingsbury, Huang et al. 2019). dmPFC and PL are also frontal cortical association areas and they have connections to M2 and ACC (Zingg, Hintiryan et al. 2014, Fillinger, Yalcin et al. 2017).

Thus, it is possible that tactile information indeed has a similar function in modulating the neural coding of social stimuli in M2 and ACCs that cannot be detected in our catFISH dataset.

4.3.3 Novel Contexts Activate Secondary Motor and Anterior Cingulate Cortices

It has been shown that animals who are left undisturbed in their home cages typically have low levels of *Arc* labelling (Guzowski, McNaughton et al. 1999, Guzowski, McNaughton et al. 2001, Guzowski, Setlow et al. 2001, Burke, Chawla et al. 2005, Burke and Barnes 2015), which is why we included the "cage control" condition in our study.

However, the levels of "foci +" cells in cage control animals in our study were in fact higher than experimental animals, which was unexpected. Coincidentally, an ongoing study in Burke Lab suggests that the ACC has elevated basal *Arc* expression compared to other typical areas they have been investigating such as medial temporal lobe structures, the striatum, and infralimbic and prelimbic cortices *(direct communication from Burke Lab)*.

This can be explained in different ways. If, for example, the *Arc* signal from cage control animals are considered as baseline activity, by logic, there may be cells which stop firing during observation of another animal in M2 and ACC. However, M2 and ACC have been shown to respond to visual stimuli (Ma, Ning et al. 2016, Ebbesen, Insanally et al. 2018, Itokazu, Hasegawa et al. 2018), and ACC is associated with observational learning (Allsop, Wichmann et al. 2018, Carrillo, Han et al. 2019), thus, a decrease in ACC activity in experimental animals does not seem to fit the data.

A more likely reason could be that M2 and ACC were activated in the cage control animals by uncontrolled stimuli approximately five minutes before the snap freezing process (described below). Subsequent correspondence with the Burke Lab supports this theory. In a typical *Arc* catFISH experiment, cage control animals are only used to confirm baseline activation. They are handled for a couple of days before the experiment and put in the isoflurane chamber in the colony room directly from their home cage *(direct communication from Burke Lab)*, which is intended to keep the baseline activity relatively uncontaminated by novel context or stimuli.

However, due to differences in protocols and rules of conduct between institutes, it was not possible to execute the snap freezing process of control animals in a similar way at the Kavli Institute. Instead, animals had to be transported through the hallway on a cart and introduced to the surgery room where snap freezing was conducted for the first time. Even though the animals were familiar and comfortable with the experimenter, they were not familiar with the room. It was assumed that since the control animals were going to be in their home cages and undisturbed during the transportation step, the process would lead to at most negligible disturbances in the baseline activation pattern. Therefore, the elevated "foci +" in control animals could be associated with exposure to the novel environment. If we assume that "foci +" levels in experimental animals were driven partly by visual information of the conspecific, the elevation of baseline activity in control animals here was even larger. It was beyond the scope of this study, but future work could be planned to quantify the effects of moving animals to a novel room against animals thoroughly routinized to such a procedure.

4.3.4 Secondary Motor and Anterior Cingulate Cortices were Activated to Differing Degrees

Arc expression was significantly different in M2, dACC and vACC of experimental animals according to the pairwise chi-square tests (M2-dACC, M2-vACC, dACC-vACC). Since “cyto +” and “foci +” levels were similar across regions, it is not unlikely that this difference was mostly driven by “both” levels, which were highest in M2 followed by dACC and vACC ($M2_{both}$>$dACC_{both}$>$vACC_{both}$) (Figure 14).

Recent studies have shown that cells in M2 have strong neural correlates for an animal’s own actions (Tombaz, Dunn et al. 2019) and posture (Mimica, Dunn et al. 2018). As the animals in the present study were freely moving, similar movements across epochs might have activated the same cells. It is tempting to explain the difference between “both” levels in M2 and ACC activation regarding motor activation, however the difference between M2 and dACC is negligible in controls (Supplemantery Figure 3) which were also freely moving. Also, microstimulation studies show involvement of rat ACC in eye and nose movements (Brecht, Krauss et al. 2004), which makes this explanation unlikely. ACC in rodents is strongly associated with nociceptive and fear related circuitry (Vogt 2015, Allsop, Wichmann et al. 2018), so in a non-threatening environment the activation induced by social interaction might be attenuated creating the difference observed in this study.

That said, dACC and vACC both receive projections from same cortical and subcortical structures (Fillinger, Yalcin et al. 2017). However, dACC generally has denser projections from areas including claustrum and parietal association areas (Figure 4), compared to vACC (Fillinger, Yalcin et al. 2017). The difference in the “both” levels between dACC and vACC can be a reflection of this asymmetry in connectivity from other association areas.

4.3.5 Similarity Scores

When doing FISH in behavioural experiments, similarity scores are calculated to reduce values for “foci +”, “cyto +”, and “both” to a single score to make it simpler to compare activation patterns across brain areas for different behavioural epochs (see Methods for a detailed explanation) (Vazdarjanova and Guzowski 2004, Burke, Chawla et al. 2005). Briefly, a similarity score closer to 1 indicates that more similar neural ensembles were activated across two distinct epochs.

M2, dACC and vACC all had high similarity scores in experimental animals (>0.5), which verifies that a similar ensemble of neurons was active during both episodes of behaviour (INT and OBS).

Typically, similarity scores for cage control animals are not calculated because of low levels of baseline activity and the absence of novel or relevant stimuli. However, in this study cage controls experienced a novel context just before sacrifice, so similarity scores for these animals were calculated to determine if this caused a shift from baseline activity.

Interestingly, the caged controls also had high similarity scores across regions, but their medians were still lower than their experimental counterparts (Figure 15). However, we deliberately chose not to go through with a statistical comparison between experimental and control cases here, as control animals did not have the exact experience minus the social interaction as experimental animals, so it was not justifiable to apply pairwise tests.

The scores for the control animals suggest that the activation by the pre-sacrifice novel environment was less similar to basal Arc expression ("cyto +" labelling) compared to that in experimental animals across the two epochs of social interaction.

Moreover in dACC and vACC, variability of similarity scores was smaller than controls while M2 scores of both conditions show similar interquartile range (Figure 15). Therefore, we can say that at least in ACC two epochs of social interaction activates highly similar neural ensembles more consistently than a shift from baseline activity caused by a random novel stimulus.

4.4 Functional Implications

To our best knowledge, in rodents M2 has not been associated with non-aversive social cognition before. In fact, recent work probing for mirror-like neurons in mice found opposing results, suggesting that the area does not show neural correlates for observed behaviour (Tombaz, Dunn et al. 2019). However, the animals in that study were not physically interacting, so behaviours were observed only in the visual modality, and any effects of social touch were unexplored.

The ACC, on the other hand, is associated with emotion regulation and neutral or positive social interactions in monkeys and humans (Frith and Frith 2001, Mundy 2003, Rudeback, Buckley et al. 2006, Somerville, Heatherton et al. 2006). However, the role of this area during positive social interactions has so far been neglected in rodent models.

Our present results—namely, the heightened levels of *Arc* expression in experimental animals—suggest that M2 and ACC are activated in the mouse brain during social interactions with a conspecific. Moreover, the social status and behaviour of the animal may have influenced the neural activity levels in the experimental animals.

However, the specific role and prominence of tactile interactions beyond visual input is unclear. Previous literature has underlined the importance of tactile interactions with a conspecific in social buffering of anxiety and fear learning (Meyza, Bartal et al. 2017), during prosocial consolation in fear conditioned mice (Allsop, Wichmann et al. 2018), and in driving neural synchrony in freely interacting animals (Kingsbury, Huang et al. 2019, Zhang and Yartsev 2019).

Therefore, it is reasonable that social touch indeed has an effect on neural representations of social interactions with a conspecific. However, since *Arc* was induced during both visual and

tactile conditions here, it is not possible to infer how and to what extent this effect occurs in our data. Determining this would likely require a re-designed paradigm, such as with light and dark sessions, if catFISH were used again to interrogate neural activity. Otherwise a different method that provides a more instantaneous readout of neural activity, such as calcium imaging or single-unit electrophysiology, will be required.

4.5 Limitations

Sample Size

Due to constraints on time and resources, and with the addition of exclusion of animals that did not fit the aim of the study due to fighting, only two animals were used per condition (experimental, cage control) which led to multiple limitations.

The most important caveat was the underrepresentation of the population and not having a dataset large enough to represent the range of variability. For example, levels of "both" labelling in experimental animals were significantly higher than those in cage control animals. However, there is a clustering of data points in experimental animals (Figure 13) with one animal (EXP2) having higher levels. While this could be genuine signals, statistical verification of this activation pattern is not possible with only two animals. It is therefore unresolved if this effect was reflective of social hierarchy, the animal's own behaviour, or one of the animals having anomalously high activity *Arc* expression. Answering these questions will require repeating the experiment with more individuals. Therefore, the results from this study are not conclusive and, accordingly, interpretation of the data should be taken with a grain of salt.

The small sample also violated the assumptions of sample size for running an ANOVA test, so a highly sensitive, but less informative, chi-square test was used. That is, the chi-square is more sensitive to small differences in the data because of the mathematical formula, but the test does not provide an explanation of where the significance emerges from. In order to prevent overestimating the statistical difference of the chi-square, an ANOVA test was also applied to reaffirm the chi-squire results even though it was not statistically valid in this context.

No Behaviourally-matched Controls

As mentioned previously, the cage control condition in this study was not similar to that typically performed in *Arc* catFISH literature, with the animals here being carted to a novel room prior to sacrifice. The fact that the animals had a novel experience before sacrifice provides a better comparison point to "foci +" and "both" labelled activation, but it also prevents us from seeing the actual baseline activity for *Arc* expression.

Inclusion of behaviourally-matched control animals that experienced similar behavioural episodes without any social interaction, and also having a cage control condition in which the

animals were previously habituated to the surgery room, would have helped further clarify how the result should be interpreted.

Lack of Counterbalanced Order

The animals that experienced the behavioural epochs in a counterbalanced order (OBS/INT) had to be excluded because of fighting. Therefore, the effect of order on representation of social interaction (or lack thereof) could not be explored, despite the original design and intention to do so.

4.6 Future Directions

Within the Same Experiment

As *Arc* in situ hybridization is done post factum, different areas of the same brains could be analysed further for comparison. For example, since dmPFC and PL cortices showed substantial synchronization of brain activity in extremely similar behavioural episodes as used here (Kingsbury, Huang et al. 2019), it is a reasonable next step to look at these areas in the tissue we have already collected.

Midcingulate cortex and posterior parts of secondary motor cortex could also be investigated to compare activation patterns, since these areas have different connectivity patterns than the more anterior regions considered here (Fillinger, Yalcin et al. 2017, Olsen, Hovde et al. 2019).

The analysis of sections from fighting animals could also help to answer some questions regarding how negative factors such as stress, anxiety and social pain affect representation of a conspecific in M2 and ACC.

Specifically, would these factors differentiate activation between M2 and ACC further as ACC is extensively implicated in nociception and observational fear learning? In considering sub-cortical areas, would the basolateral amygdala and ACC have had distinguishable “foci +” and “cyto +” from each other, or from corresponding areas in prosocially interacting cohorts? What about comparisons to determine if the ACC (implicated in prosocial behaviour) and ventromedial hypothalamus (which mediates aggression*;* (Lin, Boyle et al. 2011)) showed differentiable patterns of activation in fighting and non-fighting animals—would the neural data alone have revealed which experience the animals had? Would the levels in fighting animals have reflected differentiated representations for aggressive tactile interaction or mere visual observation?

Lastly, would there have been differences in activation patterns reflecting the behavioural status or hierarchy of the animals as we may have found in the experimental animals in this study?

With the Same Method

As mentioned before, one of the key limitations of this study was the absence of multiple experimental groups including a group with counterbalanced epoch order. These groups can be made up of multiple orders of behavioural episodes that would have helped disambiguate the results. One major step would be to compare an epoch to itself along with the other one, such as INT/OBS and INT/INT. Another key addition would have been the inclusion of truly behaviourally matched controls, in which animals would go through the same experience in the experimental cage but without the presence of a conspecific.

To probe more deeply whether elevated levels of "both" labelling in experimental animals was caused by novel experience rather than social interaction with a conspecific, toys or 3D printed models of animals could be used in a separate condition. This would be interesting since existing bodies of work have shown that rodents are adept at distinguishing true conspecifics from inanimate look-alikes. For example, a study on empathy in rats showed that they would open a trap door to release a conspecific but not a toy rat (Bartal, Decety et al. 2011). Another study on aggression in virgin male mice used silicone models of pups with increasing recognisability to investigate the effect of morphology vs. chemical signals on the phenomena (Isogai, Wu et al. 2018). The aggression was strongest toward a dead pup but the model also induced similar bouts of aggression which declined with decreasing recognisability of the model. Chemical signals combined with morphology resulted in substantial aggression. Similar models can be used in the context of this study for a comparison in conditions such as INT_{model}/INT_{animal}, OBS_{model}/OBS_{animal}, INT_{model}/OBS_{animal} or any combination of these epochs.

Another point to investigate could include sex differences. In this study we used male animals because of their prevalent usage in previous ACC literature on observational fear learning (Allsop, Wichmann et al. 2018, Carrillo, Han et al. 2019). However, female and male animals show behavioural differences in specific social contexts and during social interactions. This notion is supported by behavioural work exploring kinship and familiarity in mice, which reported no aggression among any juvenile or adult female pairs, while interaction with a conspecific, including touch, was at similar or higher levels than male pairs (Kareem and Barnard 1982). Moreover, first-hand observations in the Kavli Institute confirm that female animals can be housed together post-operatively without fighting since their levels of aggression toward each other are generally lower than in males.

It has been shown that locomotor behaviour and self-motion increase firing rates and enhance tuning in multiple brain regions including anterodorsal thalamus and visual cortex (Zugaro, Tabuchi et al. 2001, Erisken, Vaiceliunaite et al. 2014, Shinder and Taube 2014). To distinguish movement or posture-related neural activation from that driven by social interactions, the animals could also be tracked using video-based software such as Deep Lab Cut. This could prove particularly helpful to disambiguate differences in "both +" labelling between experimental animals.

Considering a Broader Context

Since the current results did not show a disassociation between tactile and visual experiences with conspecifics, it appears that more precise tools must be employed to further investigate the neural coding of social interactions in animals. As noted above, depending on the brain area studied and the animal model used, electrophysiology or calcium imaging would be powerful tools to bear in studying neural ensembles in such experiments.

Social interactions might be encoded in ways that FISH cannot detect, such as synchronization of brain activity (Kingsbury, Huang et al. 2019, Zhang and Yartsev 2019), which requires precise temporal resolution as opposed to the method used in this study, or the same cells might be driven during visual and tactile interactions with the same animal.

Real time recordings would also provide a way to explore the modulation of an animal's own behaviour during ongoing episodes of social interactions.

Once areas of interest were identified, the subsequent manipulation of these areas with genetic tools would allow us to determine if these areas are essential for specific aspects of social behaviour.

Chapter 5

Conclusion

The aim of this study was to explore if cell ensembles in M2 and ACC of the mouse brain showed differential activation patterns for social contexts involving tactile interaction or those that were limited to visual input. Secondary aims of the study included investigating involvement of these areas (especially ACC) in positive social interaction in freely moving animals in a naturalistic setting without the need for behavioural training, surgical interventions or conditioning.

The results from experimental animals did not reveal a disassociation of activation for the two behavioural episodes (INT, OBS) in either M2 or ACC, but showed an overall increase in activation of cell populations in experimental animals. This suggests that these areas respond to a conspecific with a general upregulation of neural activity. However, tactile interaction might have a yet-to-be-discovered role in the representation of social interactions in these areas that was not possible to detect using a FISH-based readout of neural activation.

The differences in scores from experimental animals suggest that there is reason to believe animal's social status or behaviour could have an effect on the activation of these areas. However, how this modulation occurs requires future investigation.

Bibliography

Allsop, S. A., R. Wichmann, F. Mills, A. Burgos-Robles, C. J. Chang, A. C. Felix-Ortiz, A. Vienne, A. Beyeler, E. M. Izadmehr, G. Glober, M. I. Cum, J. Stergiadou, K. K. Anandalingam, K. Farris, P. Namburi, C. A. Leppla, J. C. Weddington, E. H. Nieh, A. C. Smith, D. Ba, E. N. Brown and K. M. Tye (2018). "Corticoamygdala Transfer of Socially Derived Information Gates Observational Learning." Cell **173**(6): 1329-1342 e1318.

Bartal, I. B.-A., J. Decety and P. Mason (2011). "Empathy and Pro-Social Behavior in Rats." Science **334**(6061): 1427.

Barthas, F. and A. C. Kwan (2017). "Secondary Motor Cortex: Where 'Sensory' Meets 'Motor' in the Rodent Frontal Cortex." Trends Neurosci **40**(3): 181-193.

Blair, K. S., M. Geraci, B. W. Smith, N. Hollon, J. DeVido, M. Otero, J. R. Blair and D. S. Pine (2012). "Reduced dorsal anterior cingulate cortical activity during emotional regulation and top-down attentional control in generalized social phobia, generalized anxiety disorder, and comorbid generalized social phobia/generalized anxiety disorder." Biol Psychiatry **72**(6): 476-482.

Bobrov, E., J. Wolfe, Rajnish P. Rao and M. Brecht (2014). "The Representation of Social Facial Touch in Rat Barrel Cortex." Current Biology **24**(1): 109-115.

Brecht, M. (2011). "Movement, Confusion, and Orienting in Frontal Cortices." Neuron **72**(2): 193-196.

Brecht, M., A. Krauss, S. Muhammad, L. Sinai-Esfahani, S. Bellanca and T. W. Margrie (2004). "Organization of rat vibrissa motor cortex and adjacent areas according to cytoarchitectonics, microstimulation, and intracellular stimulation of identified cells." Journal of Comparative Neurology **479**(4): 360-373.

Bruce, C. J. and M. E. Goldberg (1985). "Primate frontal eye fields. I. Single neurons discharging before saccades." Journal of Neurophysiology **53**(3): 603-635.

Burke, S. N. and C. A. Barnes (2015). "The neural representation of 3-dimensional objects in rodent memory circuits." Behav Brain Res **285**: 60-66.

Burke, S. N., M. K. Chawla, M. R. Penner, B. E. Crowell, P. F. Worley, C. A. Barnes and B. L. McNaughton (2005). "Differential encoding of behavior and spatial context in deep and superficial layers of the neocortex." Neuron **45**(5): 667-674.

Bush, G., P. Luu and M. I. Posner (2000). "Cognitive and Emotiona Influences in Anterior Cingulate Cortex." Trends in Cognitive Sciences **4**(6): 215-222.

Calhoun, J. B. (1963). The ecology and sociology of the Norway rat. Bethesda, Md., U.S. Dept. of Health, Education, and Welfare, Public Health Service; [for sale by the Superintendent of Documents, U.S. Govt. Print. Off.].

Cao, V. Y., Y. Ye, S. Mastwal, M. Ren, M. Coon, Q. Liu, R. M. Costa and K. H. Wang (2015). "Motor Learning Consolidates Arc-Expressing Neuronal Ensembles in Secondary Motor Cortex." Neuron **86**(6): 1385-1392.

Carrillo, M., Y. Han, F. Migliorati, M. Liu, V. Gazzola and C. Keysers (2019). "Emotional Mirror Neurons in the Rat's Anterior Cingulate Cortex." Curr Biol **29**(8): 1301-1312 e1306.

Dapretto, M., M. S. Davies, J. H. Pfeifer, A. A. Scott, M. Sigman, S. Y. Bookheimer and M. Iacoboni (2006). "Understanding emotions in others: mirror neuron dysfunction in children with autism spectrum disorders." Nature Neuroscience **9**(1): 28-30.

Davis, S., B. Bozon and S. Laroche (2003). "How necessary is the activation of the immediate early gene zif268 in synaptic plasticity and learning?" Behavioural Brain Research **142**(1-2): 17-30.

Deffeyes, J. E., B. Touvykine, S. Quessy and N. Dancause (2015). "Interactions between rostral and caudal cortical motor areas in the rat." J Neurophysiol **113**(10): 3893-3904.

Devinsky, O., M. J. Morrel and B. A. Vogt (1995). "Contributions of Anterior Cingulate Cortex to Behaviour." Brain **118**: 279-306.

di Pellegrino, G., L. Fadiga, L. Fogassi, V. Gallese and G. Rizzolatti (1992). "Understanding motor events: a neurophysiological study." Experimental Brain Research **91**(1): 176-180.

Ebbesen, C. L., M. N. Insanally, C. D. Kopec, M. Murakami, A. Saiki and J. C. Erlich (2018). "More than Just a “Motor”: Recent Surprises from the Frontal Cortex." The Journal of Neuroscience **38**(44): 9402.

Erisken, S., A. Vaiceliunaite, O. Jurjut, M. Fiorini, S. Katzner and L. Busse (2014). "Effects of Locomotion Extend throughout the Mouse Early Visual System." Current Biology **24**(24): 2899-2907.

Erlich, Jeffrey C., M. Bialek and Carlos D. Brody (2011). "A Cortical Substrate for Memory-Guided Orienting in the Rat." Neuron **72**(2): 330-343.

Etkin, A., T. Egner and R. Kalisch (2011). "Emotional processing in anterior cingulate and medial prefrontal cortex." Trends Cogn Sci **15**(2): 85-93.

Ferrari, P. F., V. Gallese, G. Rizzolatti and L. Fogassi (2003). "Mirror neurons responding to the observation of ingestive and communicative mouth actions in the monkey ventral premotor cortex." European Journal of Neuroscience **17**(8): 1703-1714.

Fillinger, C., I. Yalcin, M. Barrot and P. Veinante (2017). "Afferents to anterior cingulate areas 24a and 24b and midcingulate areas 24a' and 24b' in the mouse." Brain Struct Funct **222**(3): 1509-1532.

Fogassi, L., P. F. Ferrari, B. Gesierich, S. Rozzi, F. Chersi and G. Rizzolatti (2005). "Parietal Lobe: From Action Organization to Intention Understanding." Science **308**(5722): 662.

Frith, U. and C. Frith (2001). "The Biological Basis of Social Interaction." Current Direction in Psychological Science **10**(5): 151-155.

Gallese, V., L. Fadiga, L. Fogassi and G. Rizzolatti (1996). "Action recognition in the premotor cortex." Brain **119**(2): 593-609.

Gallese, V., C. Keysers and G. Rizzolatti (2004). "A unifying view of the basis of social cognition." Trends Cogn Sci **8**(9): 396-403.

Guzowski, J. F., G. L. Lyford, G. D. Stevenson, F. P. Houston, J. L. McGaugh, P. F. Worley and C. A. Barnes (2000). "Inhibition of Activity-Dependent Arc Protein Expression in the Rat Hippocampus Impairs the Maintenance of Long-Term Potentiation and the Consolidation of Long-Term Memory." **20**(11): 3993-4001.

Guzowski, J. F., B. L. McNaughton, C. A. Barnes and P. F. Worley (1999). "Environment-specific expression of the immediate-early gene Arc in hippocampal neuronal ensembles." Nature Neuroscience **2**(12): 1120-1124.

Guzowski, J. F., B. L. McNaughton, C. A. Barnes and P. F. Worley (2001). "Imaging neural activity with temporal and cellular resolution using FISH." Current Opinion in Neurobiology **11**(5): 579-584.

Guzowski, J. F., B. Setlow, E. K. Wagner and J. L. McGaugh (2001). "Experience-Dependent Gene Expression in the Rat Hippocampus after Spatial Learning: A Comparison of the Immediate-Early GenesArc, c-fos, and zif268." **21**(14): 5089-5098.

Hernandez, A. R., J. E. Reasor, L. M. Truckenbrod, K. T. Campos, Q. P. Federico, K. E. Fertal, K. N. Lubke, S. A. Johnson, B. J. Clark, A. P. Maurer and S. N. Burke (2018). "Dissociable effects of advanced age on prefrontal cortical and medial temporal lobe ensemble activity." Neurobiol Aging **70**: 217-232.

Hill, Daniel N., John C. Curtis, Jeffrey D. Moore and D. Kleinfeld (2011). "Primary Motor Cortex Reports Efferent Control of Vibrissa Motion on Multiple Timescales." Neuron **72**(2): 344-356.

Hirata, S. (2009). "Chimpanzee social intelligence: selfishness, altruism, and the mother–infant bond." Primates **50**(1): 3-11.

Hovde, K., M. Gianatti, M. P. Witter and J. R. Whitlock (2019). "Architecture and organization of mouse posterior parietal cortex relative to extrastriate areas." Eur J Neurosci **49**(10): 1313-1329.

Iacoboni, M. (2009). "Imitation, Empathy, and Mirror Neurons." Annual Review of Psychology **60**(1): 653-670.

Iacoboni, M. and M. Dapretto (2006). "The mirror neuron system and the consequences of its dysfunction." Nature Reviews Neuroscience **7**(12): 942-951.

Isogai, Y., Z. Wu, M. I. Love, M. H.-Y. Ahn, D. Bambah-Mukku, V. Hua, K. Farrell and C. Dulac (2018). "Multisensory Logic of Infant-Directed Aggression by Males." Cell **175**(7): 1827-1841.e1817.

Itokazu, T., M. Hasegawa, R. Kimura, H. Osaki, U. R. Albrecht, K. Sohya, S. Chakrabarti, H. Itoh, T. Ito, T. K. Sato and T. R. Sato (2018). "Streamlined sensory motor communication through cortical reciprocal connectivity in a visually guided eye movement task." Nat Commun **9**(1): 338.

Kareem, A. M. and C. J. Barnard (1982). "The Importance of Kinship and Familiarity in Social Interactions Between Mice." Animal Behavior **30**: 594-601.

Kingsbury, L., S. Huang, J. Wang, K. Gu, P. Golshani, Y. E. Wu and W. Hong (2019). "Correlated Neural Activity and Encoding of Behavior across Brains of Socially Interacting Animals." Cell **178**(2): 429-446.e416.

Knapska, E., M. Mikosz, T. Werka and S. Maren (2010). "Social modulation of learning in rats." Learn Mem **17**(1): 35-42.

Kunicki, C., C. M. R, M. Pais-Vieira, A. Salles Cunha Peres, E. Morya and A. L. N. M (2019). "Frequency-specific coupling in fronto-parieto-occipital cortical circuits underlie active tactile discrimination." Sci Rep **9**(1): 5105.

Lin, D., M. P. Boyle, P. Dollar, H. Lee, E. S. Lein, P. Perona and D. J. Anderson (2011). "Functional identification of an aggression locus in the mouse hypothalamus." Nature **470**: 221.

Ma, L.-q., L. Ning, Z. Wang and Y.-W. Wang (2016). "Visual and noxious electrical stimulus-evoked membrane-potential responses in anterior cingulate cortical neurons." Molecular Brain **9**.

Masserman, J. H., S. Wechkin and W. Terris (1964). ""ALTRUISTIC" BEHAVIOR IN RHESUS MONKEYS." American Journal of Psychiatry **121**(6): 584-585.

Meyza, K. Z., I. B. Bartal, M. H. Monfils, J. B. Panksepp and E. Knapska (2017). "The roots of empathy: Through the lens of rodent models." Neurosci Biobehav Rev **76**(Pt B): 216-234.

Miller, M. W. and B. A. Vogt (1984). "Direct connections of rat visual cortex with sensory, motor, and association cortices." Journal of Comparative Neurology **226**(2): 184-202.

Mimica, B., B. A. Dunn, T. Tombaz, V. P. T. N. C. S. Bojja and J. R. Whitlock (2018). "Efficient cortical coding of 3D posture in freely behaving rats." **362**(6414): 584-589.

Mohajerani, M. H., A. W. Chan, M. Mohsenvand, J. LeDue, R. Liu, D. A. McVea, J. D. Boyd, Y. T. Wang, M. Reimers and T. H. Murphy (2013). "Spontaneous cortical activity alternates between motifs defined by regional axonal projections." Nature Neuroscience **16**: 1426.

Mundy, P. (2003). "Annotation: The neural basis of social impairments in autism: the role of the dorsal medial-frontal cortex and anterior cingulate system." Journal of Child Psychology and Psychiatry **44**(6): 793-809.

Murakami, M., M. I. Vicente, G. M. Costa and Z. F. Mainen (2014). "Neural antecedents of self-initiated actions in secondary motor cortex." Nat Neurosci **17**(11): 1574-1582.

Nakayasu, T. and K. Kato (2011). "Is full physical contact necessary for buffering effects of pair housing on social stress in rats?" Behavioural Processes **86**(2): 230-235.

Okuno, H. (2011). "Regulation and function of immediate-early genes in the brain: beyond neuronal activity markers." Neurosci Res **69**(3): 175-186.

Olsen, G. M., K. Hovde, H. Kondo, T. Sakshaug, H. H. Sømme, J. R. Whitlock and M. P. Witter (2019). "Organization of Posterior Parietal–Frontal Connections in the Rat." Frontiers in Systems Neuroscience **13**: 38.

Paus, T. (1996). "Location and function of the human frontal eye-field: A selective review." Neuropsychologia **34**(6): 475-483.

Paxinos and Franklin (2012) The mouse brain in stereotaxic coordinates. Academic Press

Pfeifer, J. H., M. Iacoboni, J. C. Mazziotta and M. Dapretto (2008). "Mirroring others' emotions relates to empathy and interpersonal competence in children." NeuroImage **39**(4): 2076-2085.

Reep, R. L., G. S. Goodwin and J. V. Corwin (1990). "Topographic organization in the corticocortical connections of medial agranular cortex in rats." Journal of Comparative Neurology **294**(2): 262-280.

Rizzolatti, G. and M. Fabbri-Destro (2008). "The mirror system and its role in social cognition." Curr Opin Neurobiol **18**(2): 179-184.

Rizzolatti, G., L. Fadiga, V. Gallese and L. Fogassi (1996). "Premotor cortex and the recognition of motor actions." Cognitive Brain Research **3**(2): 131-141.

Rizzolatti, G. and G. Luppino (2001). "The Cortical Motor System." Neuron **31**(6): 889-901.

Robinson, D. A. and A. F. Fuchs (1969). "Eye movements evoked by stimulation of frontal eye fields." Journal of Neurophysiology **32**(5): 637-648.

Rotge, J. Y., C. Lemogne, S. Hinfray, P. Huguet, O. Grynszpan, E. Tartour, N. George and P. Fossati (2015). "A meta-analysis of the anterior cingulate contribution to social pain." Soc Cogn Affect Neurosci **10**(1): 19-27.

Rudeback, P. H., M. E. Buckley, M. E. Walton and M. F. S. Rushworth (2006). "A Role for the Macaque Anterior Cingulate Gyrus in Social Valuation." Science **313**(5791): 1310-1312.

Shepherd, J. D., G. Rumbaugh, J. Wu, S. Chowdhury, N. Plath, D. Kuhl, R. L. Huganir and P. F. Worley (2006). "Arc/Arg3.1 Mediates Homeostatic Synaptic Scaling of AMPA Receptors." Neuron **52**(3): 475-484.

Shinder, M. E. and J. S. Taube (2014). "Self-motion improves head direction cell tuning." Journal of neurophysiology **111**(12): 2479-2492.

Smith, M. L., A. T. Walcott, M. M. Heinricher and A. E. Ryabinin (2017). "Anterior Cingulate Cortex Contributes to Alcohol Withdrawal- Induced and Socially Transferred Hyperalgesia." eNeuro **4**(4).

Somerville, L. H., T. F. Heatherton and W. M. Kelley (2006). "Anterior cingulate cortex responds differentially to expectancy violation and social rejection." Nat Neurosci **9**(8): 1007-1008.

Sul, J. H., S. Jo, D. Lee and M. W. Jung (2011). "Role of rodent secondary motor cortex in value-based action selection." Nat Neurosci **14**(9): 1202-1208.

Tombaz, T., B. A. Dunn, K. Hovde, R. J. Cubero, B. Mimica, P. Mamidanna, Y. Roudi and J. R. Whitlock (2019). "Action representation in the mouse parieto-frontal network." 646414.

Umiltà, M. A., L. Escola, I. Intskirveli, F. Grammont, M. Rochat, F. Caruana, A. Jezzini, V. Gallese and G. Rizzolatti (2008). "When pliers become fingers in the monkey motor system." Proceedings of the National Academy of Sciences **105**(6): 2209.

Vazdarjanova, A. and J. F. Guzowski (2004). "Differences in Hippocampal Neuronal Population Responses to Modifications of an Environmental Context: Evidence for Distinct, Yet Complementary, Functions of CA3 and CA1 Ensembles." **24**(29): 6489-6496.

Voelkl, B. and L. Huber (2007). "Imitation as Faithful Copying of a Novel Technique in Marmoset Monkeys." PloS one **2**: e611.

Vogt, B. A. (2015). Cingulate Cortex and Pain Architecture. The Rat Nervous System**:** 575-599.

Vogt, B. A., D. M. Finch and C. R. Olson (1992). "Functional Heterogeneity in Cingulate Cortex: The Anterior Executive and Posterior Evaluative Regions." Cerebral Cortex **2**(6): 435-443.

Vogt, B. A., P. R. Hof, K. Zilles, L. J. Vogt, C. Herold and N. Palomero-Gallagher (2013). "Cingulate area 32 homologies in mouse, rat, macaque and human: cytoarchitecture and receptor architecture." J Comp Neurol **521**(18): 4189-4204.

Vogt, B. A. and M. W. Miller (1983). "Cortical connections between rat cingulate cortex and visual, motor, and postsubicular cortices." **216**(2): 192-210.

Vogt, B. A. and G. Paxinos (2014). "Cytoarchitecture of mouse and rat cingulate cortex with human homologies." Brain Struct Funct **219**(1): 185-192.

Wise, S. P. (1985). "The Primate Premotor Cortex: Past, Present, and Preparatory." Annual Review of Neuroscience **8**: 1-19.

Yamawaki, N., J. Radulovic and G. M. Shepherd (2016). "A Corticocortical Circuit Directly Links Retrosplenial Cortex to M2 in the Mouse." J Neurosci **36**(36): 9365-9374.

Zhang, W. and M. M. Yartsev (2019). "Correlated Neural Activity across the Brains of Socially Interacting Bats." Cell **178**(2): 413-428.e422.

Zingg, B., H. Hintiryan, L. Gou, M. Y. Song, M. Bay, M. S. Bienkowski, N. N. Foster, S. Yamashita, I. Bowman, A. W. Toga and H.-W. Dong (2014). "Neural networks of the mouse neocortex." Cell **156**(5): 1096-1111.

Zohar, O. and J. Terkel (1991). "Acquisition of pine cone stripping behaviour in black rats (Rattus rattus)." International Journal of Comparative Psychology **5**(1): 1-6.

Zugaro, M. B., E. Tabuchi, C. Fouquier, A. Berthoz and S. I. Wiener (2001). "Active Locomotion Increases Peak Firing Rates of Anterodorsal Thalamic Head Direction Cells." Journal of Neurophysiology **86**(2): 692-702.

APPENDIX

Appendix A – Vendor List for chemicals, reagents, etc.

Isopentane (Sigma Aldritch)

Isoflurane (VWR)

RNAse Away (ThermoFisher)

Ultra-pure nuclease free water (Thermo Sci)

Paraformaldehyde (Burke)

Phosphate Buffered Saline

DAPI (ThermoFisher)

Vectashield (Vector Labs)

Riboprobe kit (Promega)

Quick spin RNA columns (Sigma Aldritch)

Dioxigenin (DIG) RNA labelling mix (Sigma Aldritch – Roche)

Saline Sodium Citrate (Fisher)

Acetic Anhydride (MP)

Acetone (Fisher)

Methanol (Fisher)

Pre-hybridization buffer (Sigma Aldritch)

Deionized nuclease free formamide (Fisher)

Hybridization buffer (sigma Aldritch)

RNAse (Qiagen)

Hydrogen Peroxide (Sigma)

Tris Buffered Saline (Invitrogen)

Tyramide signal amplification (TSA) blocking buffer (Perkin Elmer)

Normal sheep serum (Sigma)

anti-DIG/HRP (Sigma)

Tween-20 (Acros)

Cy3 (Perkin Elmer)

Prolong Gold (Invitrogen)

Appendix B – Solution recipes

Paraformaldehyde 4%

250 ml UV treated nuclease free H_2O

4 gr sodium phosphate monobasic

1.1 gr sodium hydroxide pellets

10 gr paraformaldehyde

Phosphate Buffered Saline (PBS)

100 ml 10X PBS

900 ml UV treated nuclease free H_2O

DAPI solution

1 µl DAPI : 1 ml PBS

Acetic Anhydride

250 ml UV treated nuclease free H_2O

2.3 gr sodium chloride

3.7 ml triethanolamine

1.25 ml acetic anhydride

Acetone methanol

125 ml acetone

125 ml methanol

Saline Sodium Citrate (SSC)

2X SSC

100 ml SSC

900 ml UV treated nuclease free H_2O

1X SSC

500 ml 2X SSC

500 ml UV treated nuclease free H_2O

0.5X SSC

500 ml 1X SSC

500 ml UV treated nuclease free H_2O

Tray Buffer – for day 1

100 ml 2X SSC

100 ml formamide

Tris Buffered Saline (TBS)

100 ml tris-HCl (7.5 pH)

900 ml UV treated nuclease free H_2O

Peroxidase

250 ml 1X SSC

500 µl 30% hydrogen peroxide

Tris Buffered Saline with 0.5% Tween-20

100 ml Tris-HCl

900 ml UV treated nuclease free H_2O

9 gr NaCl

500 µl Tween-20

Cy3

1:50

Cy3:Diluent from Cy3 kit

Appendix C – FISH protocols

From Burke Lab's protocols

RT – room temperature

DAPI Staining

4% PFA	10 minute	On ice, Fume hood
1X PBS	Dip x 3	RT, Fume hood
1X PBS	5 minute	RT
DAPI (110 µL per slide) Coverslip 24x55	30 minute	RT, In foil wrapped PBS tray
1X PBS	5 minute	RT
1X PBS	5 minute	RT
Vectashield (1-2 drop per slide) 24x50 coverslip	24-48 hours	RT, In foil wrapped tray

In situ hybridization

Day 1

4% PFA	5 minute	RT, Fume hood
2X SSC	2 minute	RT, Fume hood
Acetic anhydride solution	10 minute	RT, Fume hood
Rinse in UV-treated water	Dip x2	RT, Fume hood
Acetone-methanol solution	5 minute	RT, Fume hood
2X SSC	5 minute	RT, Fume hood
Pre-hybridization	30 minute	RT, on bench
Hybridization	Ca. 18 hours	56^{o}C oven

Day 2

2X SSC	5 minute	RT, rotation
2X SSC	10 minute	RT, rotation
RNase treatment in 2X SSC	15 minute	37^{o}C, oven
2X SSC	10 minute	RT, rotation
0.5X SSC	10 minute	RT, rotation
0.5X SSC	30 minute	55^{o}C, oven
0.5X SSC	5 minute	RT, rotation
1X SSC and 2% H_2O_2	15 minute	RT, rotation
1X SSC	5 minute	RT, rotation
1X SSC	5 minute	RT, rotation
1X TBS	5 minute	RT, rotation
Block with sheep serum	30 minute	RT, on bench (in tray)
Immunodetection (anti-DIG)	Ca. 18 hour	4^{o}C fridge (in tray)

Day 3

TBS-T	10 minute	RT, rotation
TBS-T	10 minute	RT, rotation
TBS-T	10 minute	RT, rotation
Detection (fluorophore Cy3)	30 minute	RT, on bench (in tray)
TBS-T	10 minute	RT, rotation
TBS-T	10 minute	RT, rotation
TBS-T	10 minute	RT, rotation
TBS	5 minute	RT, rotation
DAPI counterstain	30 minute	RT, on bench (in tray)
TBS	10 minute	RT, rotation
Coverslip with ProlongGold		

Appendix D – Software Used for Data Collection and Analysis

Adobe Illustrator CC 2018

Adobe Photoshop CC 2018

Fiji App (version 1.51h)

Keyence imaging plugin BZ-H4XD

ImageJ (version 1.52a)

Matlab R2018a

Minitab 18

ZEN 2.3 (blue edition)

Appendix E – Supplementary Material

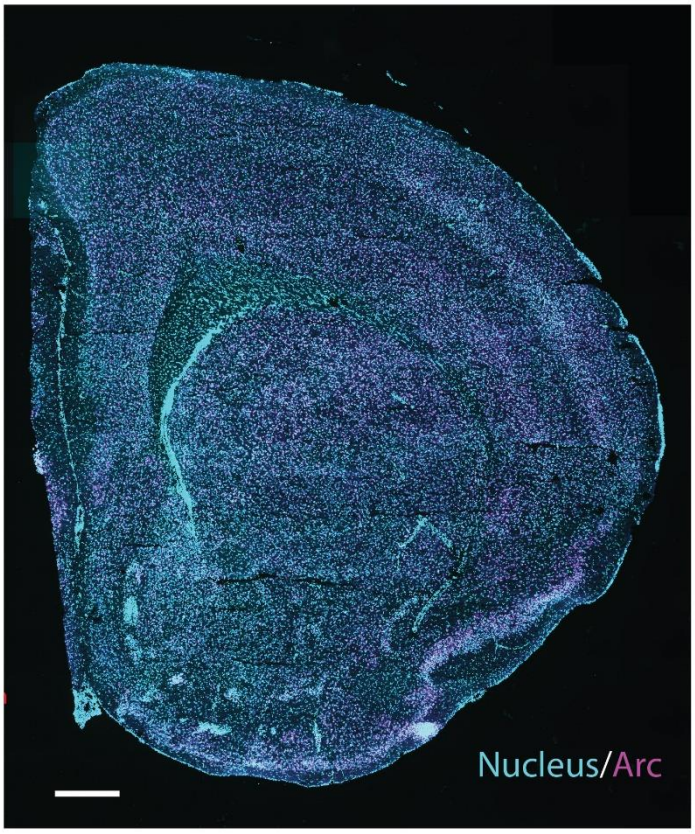

Supplementary Figure 1 Maximum electroconvulsive shock induced Arc expression

MECS induced Arc expression. Arc in magenta and nuclei cyan. Scale bar = 500 µm

A

a.1

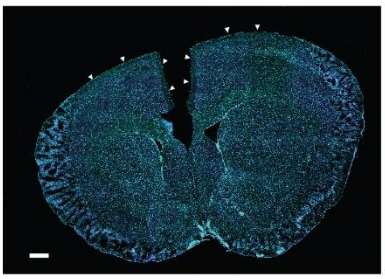

B 1.10
B 0.74

a.2

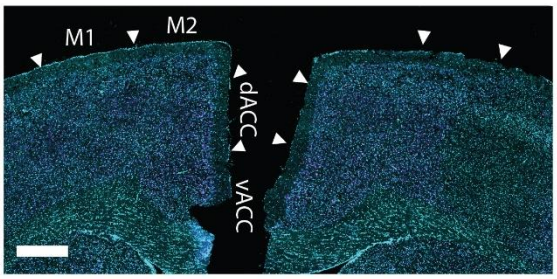

b.1

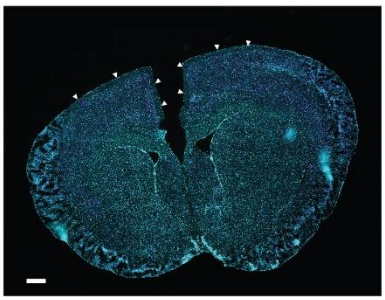

B 1.10
B 0.74

b.2

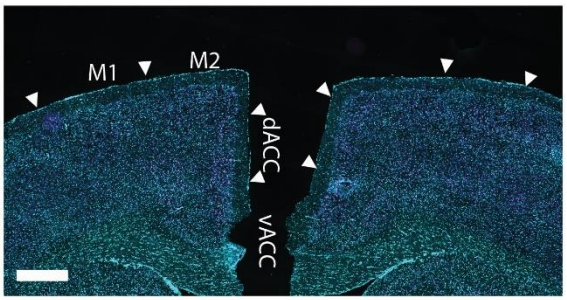

c.1

B 0.98
B 0.52

c.2

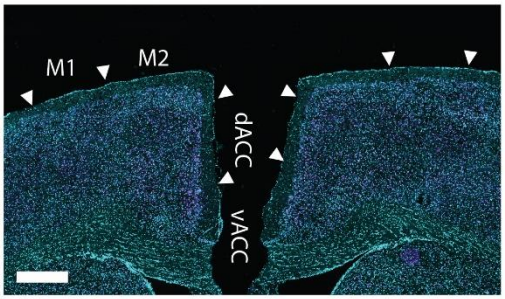

B

a.1

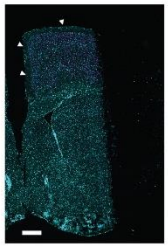

B 0.98

a.2

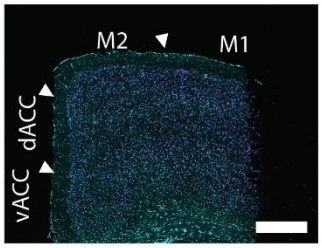

b.1

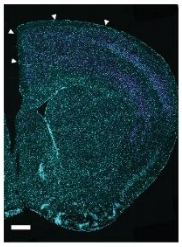

B 0.98

b.2

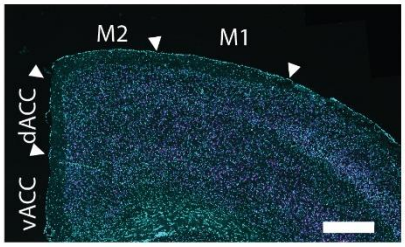

c.1

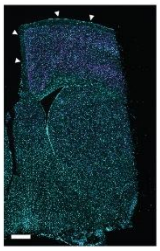

B 0.74

c.2

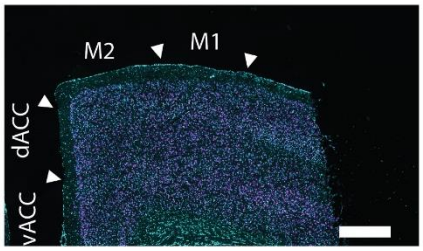

C

a.1

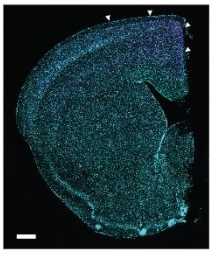

B 0.74

a.2

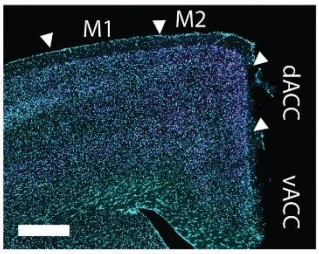

b.1

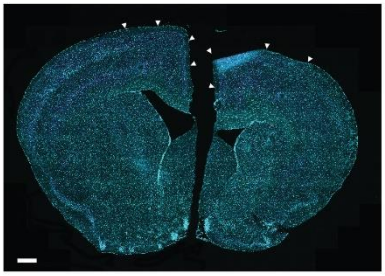

B 0.62
B 0.98

b.2

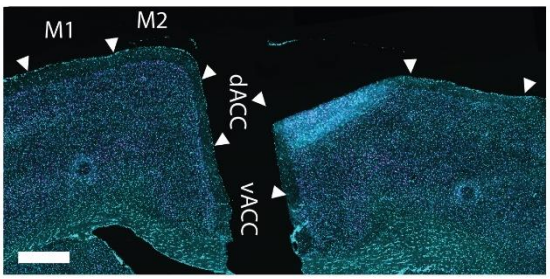

c.1

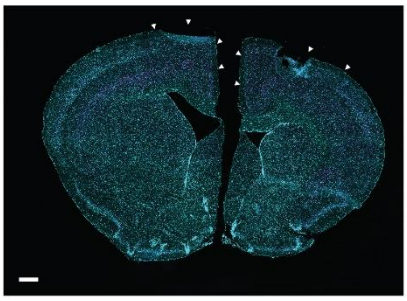

B 0.50
B 0.86

c.2

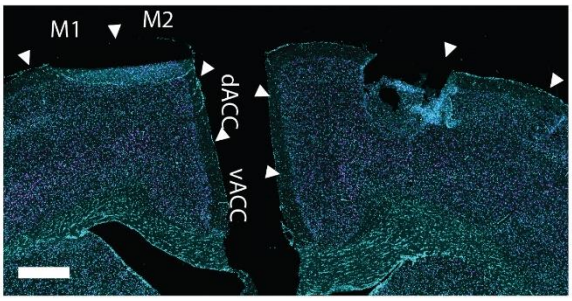

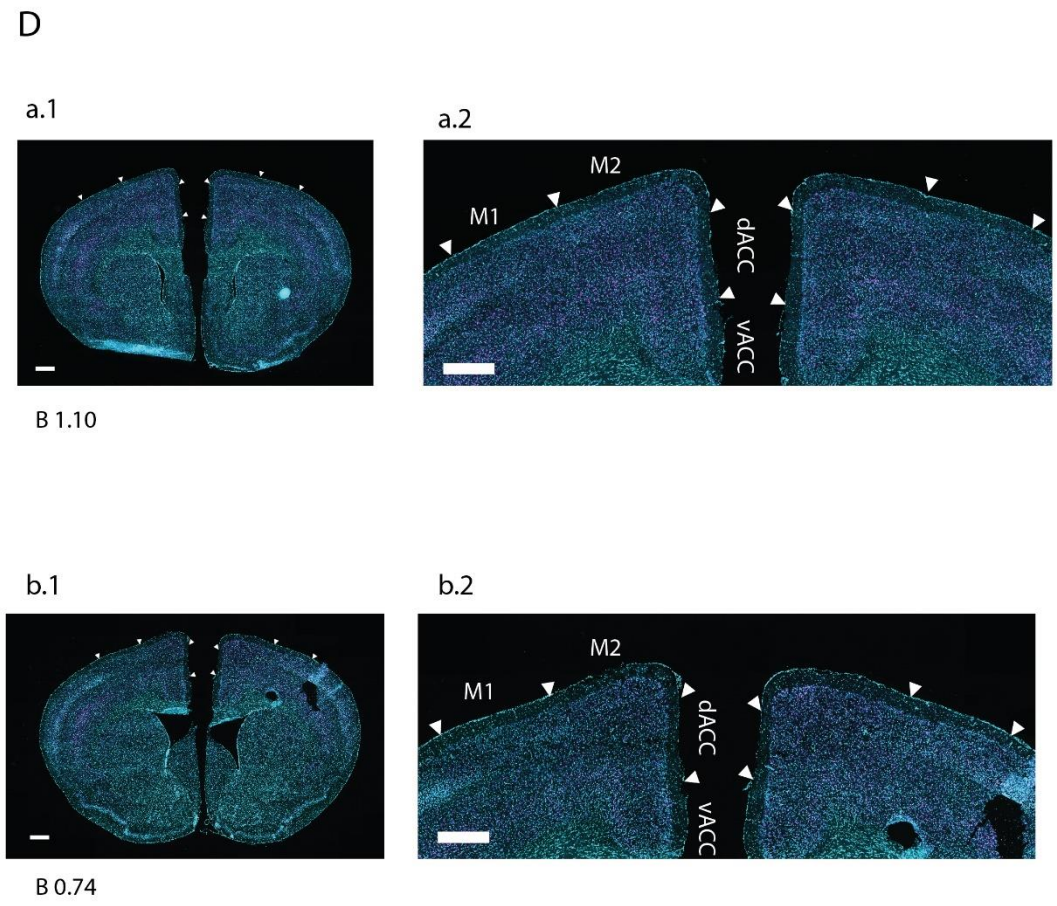

Supplementary Figure 2 Delineations of M2, dACC and vACC areas for image collection

A. and **B.** Sections from cage control animals. **C.** and **D.** Sections from experimental animals.

Arc signal is magenta and nuclei are cyan in every panel. Bregma levels are noted below left panels. Scale bars = 500 µm

Some brains were damaged during snap freezing and cryosectioning process.

	df	Sum Sq	F-value	Pr(>F)
Condition	1	17.01	1.30	$2.567e^{-01}$
Region	2	70.24	2.68	$7.225e^{-02}$
Category	2	9399.47	358.13	$1.284e^{-56}$
Condition*Region	2	13.87	0.53	$5.906e^{-01}$
Condition*Category	2	614.22	23.4	$1.583e^{-09}$
Category*Region	4	114.20	2.18	$7.466e^{-02}$
Condition*Region*Category	4	54.28	1.03	$3.918e^{-01}$
Residuals	144	1889.71		

Categories	Meandiff	Lower	Upper	Reject
Foci - Cyto	10.04	8.14	11.939	True
Foci - Both	-8.60	-10.50	-6.70	True
Cyto - Both	-18.64	-20.54	-16.74	True

Groups	Meandiff	Lower	Upper	Reject
CCFoci - ExpFoci	-3.94	-6.85	-1.03	True
CCCyto - ExpCyto	0.3	-2.6	3.21	False
CCBoth - ExpBoth	5.58	2.67	8.49	True

Supplementary Table 1 ANOVA tables for experimental vs control animals

Top - ANOVA table for experimental vs control animals. For highlighted conditions p<0.05

Middle – Tukey HSD for Arc signal category. FWER=0.05

Arc signal categories are independent from each other and their levels are drastically different across brain regions and conditions.

Bottom – Tukey HSD for the interaction effect of condition and *Arc* signal category. FWER=0.05

“Cyto +” is similar between conditions.

“Foci +” is higher in control animals than experimentals.

“Both” is higher in experimental animals than controls.

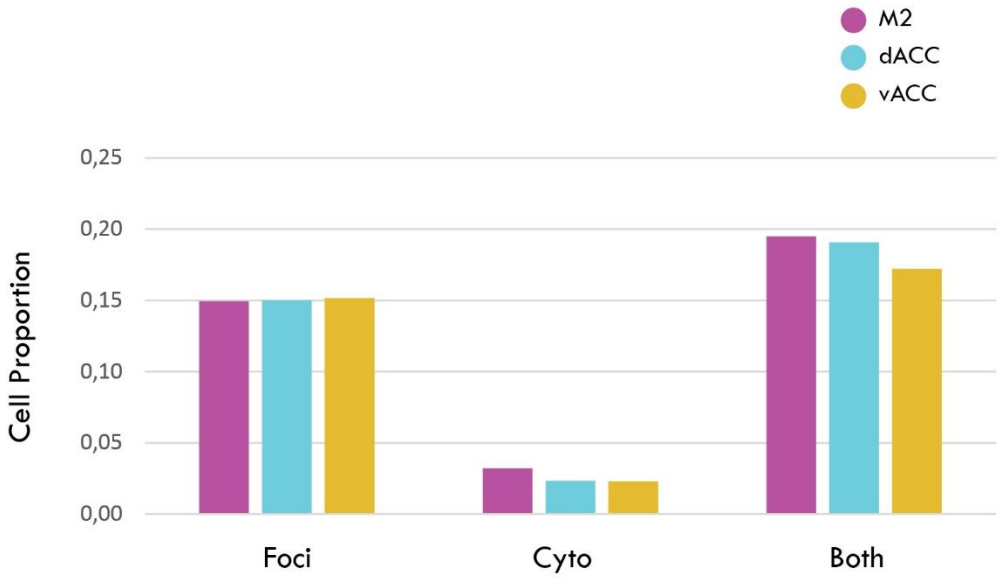

Supplementary Figure 3 Cell proportions of Arc signal categories in cage control animals

Proportions of Arc signal categories across brain regions investigated in cage control animals. Pairwise tests were not applied for cage controls. The figure was included for visual comparison.

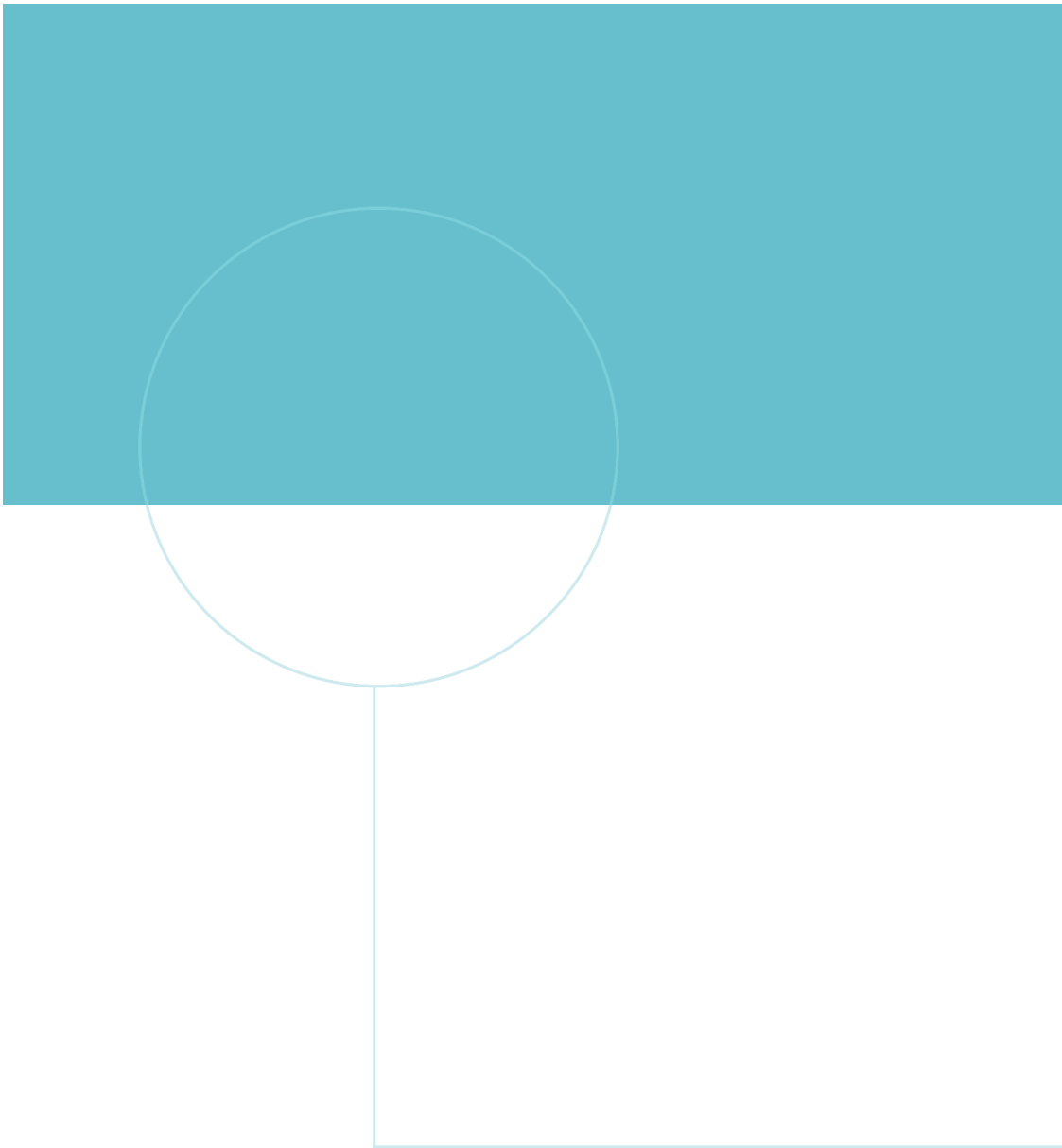

NTNU
Norwegian University of
Science and Technology